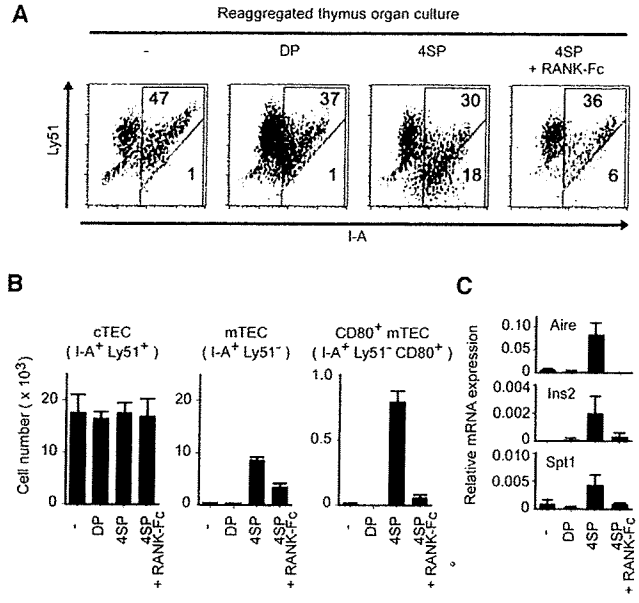

Figure 7. RANKL Produced by SP Thymocytes Promotes mTEC Cellularity in Reaggregated Thymus Organ Culture

dGuo-treated fetal thymic stromal cells (2.5×10^5) were reaggregated with equal numbers of either DP thymocytes from *Tcra*$^{-/-}$ mice or CD4SP thymocytes from B6 mice and organ cultured for 5 days. Where indicated, organ cultures included 5 μg/ml of RANK-Fc fusion protein. Cells were analyzed by flow cytometry (A and B) or quantitative RT-PCR (C).

(A) Representative two-color flow cytometry profiles for I-A and Ly51 of CD45$^-$ nonleukocytes. Numbers indicate frequency of cells within indicated areas.

(B) Numbers of indicated TEC populations per reaggregated thymus organ culture. Averages and standard errors (n = 4–5) are shown.

(C) Quantitative RT-PCR analysis of indicated genes. mRNA expression was normalized to GAPDH mRNA, and those in CD45$^-$I-A$^+$UEA1$^+$ mTECs isolated from adult thymus were arbitrarily set to 1. Averages and standard errors of 4–5 independent measurements are shown.

formation of thymic medulla containing Aire-expressing mTECs. In the absence of positive selection, not only is T lymphocyte development arrested at the DP thymocyte stage, but medulla formation is impaired as well. Through gene-expression analysis of positively selected thymocytes and thymic epithelial cells, we found that RANKL is produced by positively selected thymocytes and that RANKL receptors, RANK and OPG, are expressed by mTECs rather than by cTECs. Mice deficient for RANKL showed a reduction in the number of mTECs, whereas mice deficient for OPG showed a large number of mTECs and a large thymic medulla. Although RANKL expression in the thymus is also detectable in TCRγδ$^+$ cells and CD4$^+$CD3$^-$ LTi cells, these cells appear dispensable for mTEC generation and medulla formation. The blockade of RANKL perturbs mTEC cellularity in normal mice, whereas forced expression of RANKL restores mTEC cellularity and medulla formation in mice lacking positive selection. These results indicate that RANKL produced by positively selected thymocytes plays a major role in the increase in the number of mTECs and the formation of thymic medulla that contains Aire-expressing mTECs.

Several studies have shown that positively selected thymocytes produce signals crucial for thymic medulla formation (Shores et al., 1991; Surh et al., 1992; Naspetti et al., 1997; Nasreen et al., 2003). However, it was unclear whether positive selection regulates the genesis or increase in number of functionally competent mTECs. The present results show that the lack of positive selection reduces the number of mTECs, whereas small numbers of mTECs detectable in mice lacking positive selection contain Aire-expressing cells and CCL21-expressing cells. Aire and CCL21 are two major molecules that are vital to the execution of thymic medulla function to induce central tolerance, by displaying a diverse set of tissue-restricted genes (Derbinski et al., 2001) and by attracting CCR7-expressing positively selected cortical thymocytes toward the medulla (Ueno et al., 2004), respectively. Indeed, our results show that mTECs generated without positive selection exhibit a gene-expression profile that is characteristic of promiscuous gene expression. These results support the notion that positive selection affects the formation of thymic medulla by promoting the increase in the number of functionally competent mTECs rather than by inducing the functional maturation of mTECs. These results also suggest that thymic medulla formation consists of two sequential processes: initial maturation of mTECs independent of positive selection and subsequent increase in the number of mTECs, which is dependent on positively selected thymocytes. Our results showing that RANKL expression in bone-marrow-derived cells causes elevated proliferation of mTECs without positive selection suggest that RANKL contributes to enhancing mTEC proliferation.

Through microarray data search for genes that are highly expressed upon positive selection, we found that the expression of eight TNFSF genes encoding LTα, TNFα, LTβ, OX40L, CD40L, FasL, CD30L, and RANKL was elevated during the differentiation of DP thymocytes into SP thymocytes. Subsequent survey of genes that are more strongly expressed in mTECs than in cTECs showed that five TNFSF ligand-receptor combinations, namely, between OX40L and OX40, between CD40L and CD40, between FasL and Fas, between CD30L and CD30, and among RANKL, RANK, and OPG, represent combinations in which the ligands are more strongly expressed in SP thymocytes than in DP thymocytes and the receptors are more strongly expressed in mTECs than in cTECs. Analysis of mTEC number and medulla formation in mice deficient for one of these molecules showed that the interaction among RANKL, RANK, and OPG critically regulates the increase in the number of mTECs that leads to medulla formation. Even though the present results obtained via mice deficient for OX40L, CD40, Fas, FasL, or CD30L did not reveal the role of these molecules in regulating mTEC cellularity or medulla formation, our study does not exclude the possibility that these molecules may also be involved in regulating medulla formation. Previous studies of the roles of LTβR (Boehm et al., 2003; Chin et al., 2003; Venanzi et al., 2007) and CD40L (Dunn et al., 1997; Clegg et al., 1997) in medulla development suggest the role of additional TNFSF ligands other than RANKL in generating normal thymic medulla. Indeed, our results indicate that the number of mTECs in RANKL-deficient mice is larger than that in TCRα-deficient or ZAP70-deficient mice, suggesting that the increase in mTEC cellularity caused by positively selected thymocytes may be additionally regulated by signals other than RANKL.

Accordingly, Akiyama et al. (2008) in this issue of *Immunity* found the cooperative roles of CD40L and RANKL in postnatal

medulla formation, by showing that mTEC development is more severely affected in mice doubly deficient for RANKL and CD40 than in RANKL-deficient mice. In CD40-deficient mice, the absolute number of mTECs is not reduced, yet the frequency of class II MHC^{lo} subsets of mTECs is reduced (Akiyama et al., 2008). Thus, the defect in mTECs is much milder in CD40-deficient mice than in RANKL-deficient mice. The reduced frequency of class II MHC^{lo} subsets of mTECs was also reported in CD40L-deficient mice (Gray et al., 2006). We think that RANKL and CD40 at least partially compensate each other but unequally contribute to mTEC development, in which RANKL and CD40L play major and minor roles, respectively.

The intrathymic expression profiles of CD40L and CD40 are somewhat similar to those of RANKL and RANK, respectively; CD40L is highly detectable in positively selected thymocytes and CD4$^+$CD3$^-$ cells, whereas CD40 is more strongly detectable in mTECs than in cTECs (Figure S6). However, unlike RANKL, CD40L is not prominently detectable in TCR$\gamma\delta^+$ cells, and unlike RANK, CD40 is also detectable in CD11c$^+$ DC (Figure S6), indicating that the expression profiles of CD40L and CD40 in the thymus are not exactly identical to those of RANKL and RANK. The unequal roles of CD40L and RANKL in the thymus are also evident from our results that, unlike the retroviral expression of RANKL, that of CD40L dramatically reduces thymocyte cellularity and does not elevate mTEC cellularity in bone marrow chimeras (Figure S7). The reduction in thymocyte cellularity was also reported in proximal *Lck* promoter driven CD40L-transgenic thymocytes (Dunn et al., 1997; Clegg et al., 1997). Thus, it appears that CD40L-overexpressing immature thymocytes are inefficient in survival and/or proliferation, further suggesting that RANKL and CD40L play unequal functions in the thymus.

Our results show that the number of mTECs is reduced in the thymus of RANKL-deficient mice, whereas the number of mTECs is increased in the thymus of OPG-deficient mice. The expression of Aire and CCL21 in mTECs is detectable either in RANKL-deficient mice or in OPG-deficient mice. These results suggest that similar to positively selected thymocytes, RANKL regulates the cellularity, rather than the genesis, of functional mTECs. We also found that in vivo blockade of RANKL by a RANK-Fc fusion protein reduces the number of mTECs in normal mice even in the presence of positive selection, whereas forced expression of RANKL in mice deficient for positive selection restores the number of mTEC and medulla formation in vivo. Our results further show that RANKL is expressed in positively selected thymocytes and in TCR-stimulated DP thymocytes. On the other hand, RANKL is produced as a transmembrane cell-surface protein and can be released as a secreted protein from cell surface (Nakashima et al., 2000). Thus, it is conceivable that positive selection of thymocytes in the thymic cortex elevates the expression of RANKL, which acts to increase the number of mTECs even if mTECs may be remotely localized from positively selected thymocytes. Positive selection also induces CCR7 expression by cortical thymocytes, thereby causing the relocation of positively selected thymocytes to the medulla where mTECs produce CCR7 ligands (Ueno et al., 2004; Kurobe et al., 2006). Thus, positive selection signals increase the expression of RANKL and CCR7, thereby directly regulating both the formation of medullary microenvironment where mTECs express RANKL receptors and the migration of positively selected thymocytes toward the medulla where mTECs express CCR7 ligands.

In agreement with our results, Rossi et al. (2007) recently reported that the number of Aire-expressing mTECs was severely reduced in RANK-deficient mice. They also reported that RANKL is produced by CD4$^+$CD3$^-$ LTi cells in the thymus and that the appearance of CD4$^+$CD3$^-$ LTi cells coincides with the appearance of Aire-expressing mTECs during embryogenesis, suggesting that RANKL-expressing CD4$^+$CD3$^-$ LTi cells induce the generation of Aire-expressing mTECs during embryogenesis (Rossi et al., 2007). Our results indeed show that among adult thymocyte subpopulations, CD4$^+$CD3$^-$ LTi cells and TCR$\gamma\delta^+$ cells, in addition to positively selected thymocytes, produce RANKL. However, our results also show that unlike mice lacking positive selection, Id2-deficient mice lacking Id2-dependent LTi cells or TCRδ-deficient mice lacking TCR$\gamma\delta^+$ cells exhibit no impairment in the number of Aire-expressing mTECs and in the formation of thymic medulla in adult mice. Thus, Id2-dependent CD4$^+$CD3$^-$ LTi cells or TCR$\gamma\delta^+$ cells are dispensable for the formation of thymic medulla containing Aire-expressing mTECs in adult thymus. It is possible that LTi cells and/or TCR$\gamma\delta^+$ cells may primarily participate in the generation of mTEC during embryogenesis rather than during postnatal period, and/or LTi cells involved in thymic medulla development may be generated independent of Id2. It is also possible that any cell type expressing RANKL may be sufficient to influence the cellularity of mTECs and that the contribution of positively selected thymocytes may be best highlighted in postnatal thymus, perhaps because SP thymocytes are present in much larger number than other RANKL-expressing cells, such as LTi and TCR$\gamma\delta$ cells.

Our results reveal a role for OPG in thymic medulla formation. OPG is an osteoclastogenesis inhibitory protein that lacks a transmembrane domain and is a secreted decoy receptor for RANKL (Mizuno et al., 1998; Theill et al., 2002). We found that similar to RANK, OPG is strongly expressed in mTECs rather than in cTECs or other cell types within the thymus. We also showed that the deficiency in OPG causes an increase in mTEC number and enlargement of the thymic medulla. These results suggest that OPG-mediated fine-tuning of RANKL availability at mTEC surface crucially regulates RANK-mediated signals in mTECs, perhaps through TRAF6 and NF-κB, to increase the number of mTECs and form thymic medulla.

In conclusion, this study shows that RANKL produced by positively selected thymocytes plays a pivotal role in increasing the number of mTECs and forming thymic medulla that contains Aire-expressing mTECs. The results demonstrate that RANKL represents a major mediator of thymic crosstalk for the formation of medullary microenvironment by positively selected thymocytes. By increasing the number of Aire-expressing mTECs through RANKL, positively selected thymocytes may pave their own way for subsequent developmental regulation in the medulla to establish central tolerance. Indeed, lymphocytes generated without RANKL fail to establish self-tolerance because these cells manifest infiltration and antibody deposition in the liver (Akiyama et al., 2008). Lymphocytes generated without both RANKL and CD40 cause more severe autoimmune phenotypes than those generated without RANKL alone, whereas lymphocytes from CD40-deficient mice exhibit no detectable autoimmunity. Therefore, the severity of autoimmunity among

these mice appears to be well correlated with the defects in mTEC development. Further studies geared toward revealing the molecular mechanisms of TEC development and thymic microenvironment formation are expected to aid in improving our understanding of and controlling diverse and self-tolerant repertoire formation of T lymphocytes.

EXPERIMENTAL PROCEDURES

Mice

C57BL/6 (B6), BALB/c, ICR, B6-*Fasl*$^{gld/gld}$, and B6-*Fas*$^{lpr/lpr}$ mice were purchased from SLC Japan. *Tnfrsf11b*$^{-/-}$ mice (Mizuno et al., 1998) were purchased from CLEA Japan. *Tcra*$^{-/-}$ (Mombaerts et al., 1992), *Zap70*$^{-/-}$ (Negishi et al., 1995), *Rag2*$^{-/-}$ (Shinkai et al., 1993), *Relb*$^{-/-}$ (Burkly et al., 1995), *Tnfsf4*$^{-/-}$ (Murata et al., 2000), *Cd40*$^{-/-}$ (Kawabe et al., 1994), *Tnfsf8*$^{-/-}$ (Blazar et al., 2004), *Tnfsf11*$^{-/-}$ (Kong et al., 1999), *H2-Ab1*$^{-/-}$ (Cosgrove et al., 1991), *B2m*$^{-/-}$ (Koller et al., 1990), *Tcrd*$^{-/-}$ (Itohara et al., 1993), *Id2*$^{-/-}$ (Yokota et al., 1999), and *Rorc*$^{-/-}$ (Sun et al., 2000) mice were previously described. Experiments with mice were performed with consent from the Animal Experimentation Committee of the University of Tokushima.

Retrovirus Infection

PCR-cloned cDNA fragments encoding an open-reading frame of mouse RANKL, OX40L, CD30L, CD40L, or FasL were cloned in the retrovirus vector pMSCV-IRES-EGFP (Nitta et al., 2006). To construct retrovirus vector expressing RANK-Fc, a cDNA fragment encoding the extracellular region of RANK (aa 1–212) was ligated with human IgG1 Fc cDNA (Zettlmeissl et al., 1990) and inserted into pMSCV-IRES-EGFP. Retroviral production and infection were performed as previously described (Ueno et al., 2005). To generate irradiation bone marrow chimeras, bone marrow cells were harvested from donor mice 4 days after intravenous administration of 5-fluorouracil (150 mg/kg). Sca1$^+$ cells were sorted and precultured in growth medium (Iscove's modified Dulbecco's medium containing 20% FCS, L-glutamine, sodium pyruvate, nonessential amino acids, penicillin, streptomycin, 50 ng/ml SCF, 50 ng/ml IL-6, and 10 ng/ml IL-3). 48 hr later, the culture medium was replaced with retroviral supernatants containing 10 μg/ml polybrene, and culture plates were centrifuged at 1000 × g for 90 min at 30°C. Cells were replenished with the growth medium, cultured overnight, and additionally infected at 24 and 48 hr. Cells were intravenously injected into lethally irradiated (9.0 Gy) recipient mice.

Thymus Section Analysis

Frozen thymuses embedded in OCT compound (Sakura Finetek) were sliced into 5 μm-thick sections and stained with hematoxylin and eosin. For multicolor confocal analysis, frozen sections were fixed with acetone and stained with the following antibodies: mTEC-specific ER-TR5 followed by Alexa Fluor 633-conjugated anti-rat IgG antibody (Molecular Probes); anti-Aire antibody (Santa Cruz) followed by FITC- or Alexa Fluor 568-conjugated anti-rabbit IgG antibody (Molecular Probes); biotinylated anti-CCL21 antibody (R&D Systems) or *Ulex europaeus* agglutinin 1 (UEA1) (Vector Laboratories) followed by Alexa Fluor 488- or Alexa Fluor 546-conjugated streptavidin (Molecular Probes). Images were analyzed with TSC SP2 confocal laser-scanning microscope and Leica Confocal software (version 2.6, Leica).

Flow Cytometry Analysis and Sorting of Thymic Stromal Cells

Multicolor flow cytometry analysis and cell sorting were performed with FACSCalibur and FACS-Vantage (BD Biosciences) as described (Ueno et al., 2005). Thymic stromal cells were prepared by digesting thymic fragments with collagenase, dispase, and DNase I (Roche), as described (Gray et al., 2002). For TEC analysis, cells were stained with allophycocyanin-conjugated antibody specific for CD45, FITC-conjugated antibody specific for I-A (or antibody specific for I-E where indicated), and biotinylated UEA1 or biotinylated antibody specific for Ly51 followed by phycoerythrin-conjugated streptavidin. For TEC sorting, CD45$^-$ cells were enriched by depleting CD45$^+$ cells with a magnetic cell sorter (Miltenyi Biotec) prior to FACS cell sorting. Monoclonal antibody specific for RANKL (BioLegend #510003) was used to detect RANKL expression on cell surface. Ki67 expression, bromodeoxyuridine (BrdU) incorporation, and TdT-mediated dUTP nick end labeling (TUNEL) were measured according to the manufacturers' instructions.

Quantitative mRNA Analysis

Total cellular RNA was reverse-transcribed with oligo-dT primer and Superscript III reverse transcriptase (Invitrogen). Real-time RT-PCR was performed with SYBR Premix Ex Taq (TaKaRa) and Light Cycler DX400 (Roche). Amplified signals were confirmed to be single bands over gel electrophoresis, and normalized to GAPDH. Primer sequences are listed in Table S2.

Reaggregated Thymus Organ Culture

Thymic stromal cells isolated from E15.5 fetal thymus lobes that were cultured for 6 days in the presence of 2-deoxyguanosine (dGuo) were reaggregated with equal numbers of either DP thymocytes isolated from adult TCRα-deficient mice or CD4SP thymocytes isolated from adult B6 mice, and organ cultured for 5 days as previously described (Ueno et al., 2005). RANK-Fc fusion protein was produced by transfected 293T cells and purified with protein A-Sepharose (Amersham-Pharmacia).

SUPPLEMENTAL DATA

Supplemental Data include seven figures and two tables and can be found with this article online at http://www.immunity.com/cgi/content/full/29/3/438/DC1/.

ACKNOWLEDGMENTS

We thank H. Kikutani, T. Yasui, K. Sugamura, N. Ishii, D. Littman, S. Fagarasan, E. Podack, I. Negishi, S. Itohara, and M. Nanno for generously providing us the mice used in this study. We thank H. Nakase, T. Ueno, and Q. Cui for critically reading the manuscript. Technical support by S. Nitta is acknowledged. This study was supported by MEXT Grant-in-Aid for Scientific Research on Priority Areas "Immunological Self" and the Mitsubishi Foundation. Y.H. is a visiting graduate student from Nagoya City University Graduate School of Medical Sciences. T.N. is a JSPS Research Fellow.

Received: December 7, 2007
Revised: April 8, 2008
Accepted: June 20, 2008
Published online: September 18, 2008

REFERENCES

Akiyama, T., Maeda, S., Yamane, S., Ogino, K., Kasai, M., Kajiura, F., Matsumoto, M., and Inoue, J. (2005). Dependence of self-tolerance on TRAF6-directed development of thymic stroma. Science *308*, 248–251.

Akiyama, T., Shimo, Y., Yanai, H., Qin, J., Ohshima, D., Maruyama, Y., Asaumi, Y., Kitazawa, J., Takayanagi, H., Penninger, J.M., et al. (2008). The tumor necrosis factor family receptors RANK and CD40 cooperatively establish the thymic medullary microenvironment and self-tolerance. Immunity *29*, this issue, 423–437.

Anderson, M.S., Venanzi, E.S., Klein, L., Chen, Z., Berzins, S.P., Turley, S.J., von Boehmer, H., Bronson, R., Dierich, A., Benoist, C., and Mathis, D. (2002). Projection of an immunological self shadow within the thymus by the aire protein. Science *298*, 1395–1401.

Bendelac, A., Matzinger, P., Seder, R.A., Paul, W.E., and Schwartz, R.H. (1992). Activation events during thymic selection. J. Exp. Med. *175*, 731–742.

Blazar, B.R., Levy, R.B., Mak, T.W., Panoskaltsis-Mortari, A., Muta, H., Jones, M., Roskos, M., Serody, J.S., Yagita, H., Podack, E.R., and Taylor, P.A. (2004). CD30/CD30 ligand (CD153) interaction regulates CD4+ T cell-mediated graft-versus-host disease. J. Immunol. *173*, 2933–2941.

Bleul, C.C., Corbeaux, T., Reuter, A., Fisch, P., Monting, J.S., and Boehm, T. (2006). Formation of a functional thymus initiated by a postnatal epithelial progenitor cell. Nature *441*, 992–996.

Boehm, T., Scheu, S., Pfeffer, K., and Bleul, C.C. (2003). Thymic medullary epithelial cell differentiation, thymocyte emigration, and the control of autoimmunity require lympho-epithelial cross talk via LTβR. J. Exp. Med. *198*, 757–769.

Bonasio, R., Scimone, M.L., Schaerli, P., Grabie, N., Lichtman, A.H., and von Andrian, U.H. (2006). Clonal deletion of thymocytes by circulating dendritic cells homing to the thymus. Nat. Immunol. *7*, 1092–1100.

Burkly, L., Hession, C., Ogata, L., Reilly, C., Marconi, L.A., Olson, D., Tizard, R., Cate, R., and Lo, D. (1995). Expression of relB is required for the development of thymic medulla and dendritic cells. Nature *373*, 531–536.

Chin, R.K., Lo, J.C., Kim, O., Blink, S.E., Christiansen, P.A., Peterson, P., Wang, Y., Ware, C., and Fu, Y.X. (2003). Lymphotoxin pathway directs thymic Aire expression. Nat. Immunol. *4*, 1121–1127.

Clegg, C.H., Rulffes, J.T., Haugen, H.S., Hoggatt, I.H., Aruffo, A., Durham, S.K., Farr, A.G., and Hollenbaugh, D. (1997). Thymus dysfunction and chronic inflammatory disease in gp39 transgenic mice. Int. Immunol. *9*, 1111–1122.

Cosgrove, D., Gray, D., Dierich, A., Kaufman, J., Lemeur, M., Benoist, C., and Mathis, D. (1991). Mice lacking MHC class II molecules. Cell *66*, 1051–1066.

Daniels, M.A., Teixeiro, E., Gill, J., Hausmann, B., Roubaty, D., Holmberg, K., Werlen, G., Hollander, G.A., Gascoigne, N.R., and Palmer, E. (2006). Thymic selection threshold defined by compartmentalization of Ras/MAPK signalling. Nature *444*, 724–729.

Derbinski, J., Schulte, A., Kyewski, B., and Klein, L. (2001). Promiscuous gene expression in medullary thymic epithelial cells mirrors the peripheral self. Nat. Immunol. *2*, 1032–1039.

Dunn, R.J., Luedecker, C.J., Haugen, H.S., Clegg, C.H., and Farr, A.G. (1997). Thymic overexpression of CD40 ligand disrupts normal thymic epithelial organization. J. Histochem. Cytochem. *45*, 129–141.

Eberl, G., Marmon, S., Sunshine, M.J., Rennert, P.D., Choi, Y., and Littman, D.R. (2004). An essential function for the nuclear receptor RORγt in the generation of fetal lymphoid tissue inducer cells. Nat. Immunol. *5*, 64–73.

Finkel, T.H., Cambier, J.C., Kubo, R.T., Born, W.K., Marrack, P., and Kappler, J.W. (1989). The thymus has two functionally distinct populations of immature $\alpha\beta^+$ T cells: one population is deleted by ligation of αβ TCR. Cell *58*, 1047–1054.

Gallegos, A.M., and Bevan, M.J. (2004). Central tolerance to tissue-specific antigens mediated by direct and indirect antigen presentation. J. Exp. Med. *200*, 1039–1049.

Gray, D.H., Chidgey, A.P., and Boyd, R.L. (2002). Analysis of thymic stromal cell populations using flow cytometry. J. Immunol. Methods *260*, 15–28.

Gray, D.H., Seach, N., Ueno, T., Milton, M.K., Liston, A., Lew, A.M., Goodnow, C.C., and Boyd, R.L. (2006). Developmental kinetics, turnover, and stimulatory capacity of thymic epithelial cells. Blood *108*, 3777–3785.

Hamazaki, Y., Fujita, H., Kobayashi, T., Choi, Y., Scott, H.S., Matsumoto, M., and Minato, N. (2007). Medullary thymic epithelial cells expressing Aire represent a unique lineage derived from cells expressing claudin. Nat. Immunol. *8*, 304–311.

Honey, K., Nakagawa, T., Peters, C., and Rudensky, A. (2002). Cathepsin L regulates $CD4^+$ T cell selection independently of its effect on invariant chain: A role in the generation of positively selecting peptide ligands. J. Exp. Med. *195*, 1349–1358.

Hsu, H., Lacey, D.L., Dunstan, C.R., Solovyev, I., Colombero, A., Timms, E., Tan, H.L., Elliott, G., Kelley, M.J., Sarosi, I., et al. (1999). Tumor necrosis factor receptor family member RANK mediates osteoclast differentiation and activation induced by osteoprotegerin ligand. Proc. Natl. Acad. Sci. USA *96*, 3540–3545.

Itohara, S., Mombaerts, P., Lafaille, J., Iacomini, J., Nelson, A., Clarke, A.R., Hooper, M.L., Farr, A., and Tonegawa, S. (1993). T cell receptor δ gene mutant mice: Independent generation of αβ T cells and programmed rearrangements of γδ TCR genes. Cell *72*, 337–348.

Kawabe, T., Naka, T., Yoshida, K., Tanaka, T., Fujiwara, H., Suematsu, S., Yoshida, N., Kishimoto, T., and Kikutani, H. (1994). The immune responses in CD40-deficient mice: Impaired immunoglobulin class switching and germinal center formation. Immunity *1*, 167–178.

Kisielow, P., Teh, H.S., Bluthmann, H., and von Boehmer, H. (1988). Positive selection of antigen-specific T cells in thymus by restricting MHC molecules. Nature *335*, 730–733.

Koller, B.H., Marrack, P., Kappler, J.W., and Smithies, O. (1990). Normal development of mice deficient in β2M, MHC class I proteins, and $CD8^+$ T cells. Science *248*, 1227–1230.

Kong, Y.Y., Yoshida, H., Sarosi, I., Tan, H.L., Timms, E., Capparelli, C., Morony, S., Oliveira-dos-Santos, A.J., Van, G., Itie, A., et al. (1999). OPGL is a key regulator of osteoclastogenesis, lymphocyte development and lymph-node organogenesis. Nature *397*, 315–323.

Kurobe, H., Liu, C., Ueno, T., Saito, F., Ohigashi, I., Seach, N., Arakaki, R., Hayashi, Y., Kitagawa, T., Lipp, M., et al. (2006). CCR7-dependent cortex-to-medulla migration of positively selected thymocytes is essential for establishing central tolerance. Immunity *24*, 165–177.

Kwan, J., and Killeen, N. (2004). CCR7 directs the migration of thymocytes into the thymic medulla. J. Immunol. *172*, 3999–4007.

Mizuno, A., Amizuka, N., Irie, K., Murakami, A., Fujise, N., Kanno, T., Sato, Y., Nakagawa, N., Yasuda, H., Mochizuki, S., et al. (1998). Severe osteoporosis in mice lacking osteoclastogenesis inhibitory factor/osteoprotegerin. Biochem. Biophys. Res. Commun. *247*, 610–615.

Mombaerts, P., Clarke, A.R., Rudnicki, M.A., Iacomini, J., Itohara, S., Lafaille, J.J., Wang, L., Ichikawa, Y., Jaenisch, R., Hooper, M.L., and Tonegawa, S. (1992). Mutations in T-cell antigen receptor genes α and β block thymocyte development at different stages. Nature *360*, 225–231.

Murata, K., Ishii, N., Takano, H., Miura, S., Ndhlovu, L.C., Nose, M., Noda, T., and Sugamura, K. (2000). Impairment of antigen-presenting cell function in mice lacking expression of OX40 ligand. J. Exp. Med. *191*, 365–374.

Murata, S., Sasaki, K., Kishimoto, T., Niwa, S., Hayashi, H., Takahama, Y., and Tanaka, K. (2007). Regulation of $CD8^+$ T cell development by thymus-specific proteasomes. Science *316*, 1349–1353.

Nakashima, T., Kobayashi, Y., Yamasaki, S., Kawakami, A., Eguchi, K., Sasaki, H., and Sakai, H. (2000). Protein expression and functional difference of membrane-bound and soluble receptor activator of NF-κB ligand: Modulation of the expression by osteotropic factors and cytokines. Biochem. Biophys. Res. Commun. *275*, 768–775.

Naspetti, M., Aurrand-Lions, M., DeKoning, J., Malissen, M., Galland, F., Lo, D., and Naquet, P. (1997). Thymocytes and RelB-dependent medullary epithelial cells provide growth-promoting and organization signals, respectively, to thymic medullary stromal cells. Eur. J. Immunol. *27*, 1392–1397.

Nasreen, M., Ueno, T., Saito, F., and Takahama, Y. (2003). In vivo treatment of class II MHC-deficient mice with anti-TCR antibody restores the generation of circulating CD4 T cells and optimal architecture of thymic medulla. J. Immunol. *171*, 3394–3400.

Negishi, I., Motoyama, N., Nakayama, K., Nakayama, K., Senju, S., Hatakeyama, S., Zhang, Q., Chan, A.C., and Loh, D.Y. (1995). Essential role for ZAP-70 in both positive and negative selection of thymocytes. Nature *376*, 435–438.

Nitta, T., Nasreen, M., Seike, T., Goji, A., Ohigashi, I., Miyazaki, T., Ohta, T., Kanno, M., and Takahama, Y. (2006). IAN family critically regulates survival and development of T lymphocytes. PLoS Biol. *4*, e103.

Philpott, K.L., Viney, J.L., Kay, G., Rastan, S., Gardiner, E.M., Chae, S., Hayday, A.C., and Owen, M.J. (1992). Lymphoid development in mice congenitally lacking T cell receptor αβ-expressing cells. Science *256*, 1448–1452.

Rossi, S.W., Jenkinson, W.E., Anderson, G., and Jenkinson, E.J. (2006). Clonal analysis reveals a common progenitor for thymic cortical and medullary epithelium. Nature *441*, 988–991.

Rossi, S.W., Kim, M.Y., Leibbrandt, A., Parnell, S.M., Jenkinson, W.E., Glanville, S.H., McConnell, F.M., Scott, H.S., Penninger, J.M., Jenkinson, E.J., et al. (2007). RANK signals from $CD4^+3^-$ inducer cells regulate development of Aire-expressing epithelial cells in the thymic medulla. J. Exp. Med. *204*, 1267–1272.

Shinkai, Y., Koyasu, S., Nakayama, K., Murphy, K.M., Loh, D.Y., Reinherz, E.L., and Alt, F.W. (1993). Restoration of T cell development in RAG-2-deficient mice by functional TCR transgenes. Science *259*, 822–825.

Shores, E.W., Van Ewijk, W., and Singer, A. (1991). Disorganization and restoration of thymic medullary epithelial cells in T cell receptor-negative scid mice:

Evidence that receptor-bearing lymphocytes influence maturation of the thymic microenvironment. Eur. J. Immunol. *21*, 1657–1661.

Sun, Z., Unutmaz, D., Zou, Y.R., Sunshine, M.J., Pierani, A., Brenner-Morton, S., Mebius, R.E., and Littman, D.R. (2000). Requirement for RORγ in thymocyte survival and lymphoid organ development. Science *288*, 2369–2373.

Surh, C.D., Ernst, B., and Sprent, J. (1992). Growth of epithelial cells in the thymic medulla is under the control of mature T cells. J. Exp. Med. *176*, 611–616.

Takahama, Y., and Nakauchi, H. (1996). Phorbol ester and calcium ionophore can replace TCR signals that induce positive selection of CD4 T cells. J. Immunol. *157*, 1508–1513.

Theill, L.E., Boyle, W.J., and Penninger, J.M. (2002). RANK-L and RANK: T cells, bone loss, and mammalian evolution. Annu. Rev. Immunol. *20*, 795–823.

Ueno, T., Saito, F., Gray, D.H., Kuse, S., Hieshima, K., Nakano, H., Kakiuchi, T., Lipp, M., Boyd, R.L., and Takahama, Y. (2004). CCR7 signals are essential for cortex-medulla migration of developing thymocytes. J. Exp. Med. *200*, 493–505.

Ueno, T., Liu, C., Nitta, T., and Takahama, Y. (2005). Development of T-lymphocytes in mouse fetal thymus organ culture. Methods Mol. Biol. *290*, 117–133.

van Ewijk, W., Shores, E.W., and Singer, A. (1994). Crosstalk in the mouse thymus. Immunol. Today *15*, 214–217.

Venanzi, E.S., Gray, D.H., Benoist, C., and Mathis, D. (2007). Lymphotoxin pathway and Aire influences on thymic medullary epithelial cells are unconnected. J. Immunol. *179*, 5693–5700.

Yokota, Y., Mansouri, A., Mori, S., Sugawara, S., Adachi, S., Nishikawa, S., and Gruss, P. (1999). Development of peripheral lymphoid organs and natural killer cells depends on the helix-loop-helix inhibitor Id2. Nature *397*, 702–706.

Zettlmeissl, G., Gregersen, J.P., Duport, J.M., Mehdi, S., Reiner, G., and Seed, B. (1990). Expression and characterization of human CD4:immunoglobulin fusion proteins. DNA Cell Biol. *9*, 347–353.

内分泌かく乱化学物質研究の世界的動向

国立医薬品食品衛生研究所
安全性生物試験研究センター
井上 達

1996年にロンドン郊外のWeybridgeで、内分泌かく乱化学物質に関する初めての国際ワークショップが開催されてから10年が過ぎ、昨2007年1年間は、さまざまな回顧と展望が語られた(2007年5月は、DDTの全面禁止につながる『沈黙の春』の著者レイチェル・カーソンの生誕100年でもあった)。この間、2002年には、WHOがグローバルアセスメントをまとめ、2005年11月には、Weybridge10周年を記念したワークショップがヘルシンキで開催され、研究の進捗状況が報告された。

本稿では、内分泌かく乱化学物質研究を、ヒトを含む野生生物が環境との間に営む生体異物相互作用と捉え、この10年間の研究のあゆみの中から、今後の研究に求められていることを述べてみたい。

Weybridgeワークショップからヘルシンキ会議まで

当時、ワニ、カメ、あるいはカモメなど種々の野生生物では、それぞれ血漿エストラジオールの減少、ヴィテロジェニン(卵黄タンパク成分)の増加、あるいは卵殻の菲薄化等、さまざまな異常生態が観察され、それがジコフォール、DDT、あるいはPCBsなどさまざまな農薬、化学物質によるものではないかと危惧され、話題になりはじめていた。これはさらに、ヒトで、尿道下裂のような小児の先天性奇形、あるいは俗にキレるといった表現で表される小児の精神神経学的な障害、さらに乳がんや前立腺がんなどの頻度の亢進などにも、関連があるものとされるに至った(図1)。

こうした中で開かれた欧州連合の主催によるWeybridge会議では、世界保健機構(WHO)と経済開発協力機構(OECD)がそれぞれ役割を決め、この問題に協力

井上 達
国立医薬品食品衛生研究所
安全性生物試験研究センター長

横浜市立大学医学部卒。東京都老人総合研究所、米国ブルックヘブン国立研究所、放射線医学総合研究所などを経て、2001年より現職。専門は、実験病理学、実験動物学、分子毒性学。現在は化学物質の生体影響発現機構の研究を進めている。著書に、「Toxicogenomics」(編著、Springer-Verlag社、2003年)など。

危惧された表徴所見	生物学的蓋然性	疫学的所見	研究課題
先天性奇形（尿道下裂など）	yes	???	発生障害の機構研究（含:胎生期ウィンドウ問題、核内受容体問題など）
生殖能の低下	yes	???	繁殖毒性障害の機構研究 化学物質とホルモン受容体の相互作用研究
精神神経学的障害	yes	???	高次生命系のかく乱の可能性（中枢神経系、内分泌系、免疫系の発生生物学）
発がん性の亢進（乳がん・前立腺がん.）	????	???	組織特異的遺伝子発現;エストロゲン・シグナル応答性遺伝子発現
野生生物所見（雌雄差、など）	yes & ???	——	感受性の種差を裏付ける機構研究（種差の特徴; 生殖腺の形態形成）
低用量反応	yes	——	受容体原性毒性反応機構
相乗／相加反応	yes	——	エストロジェンシグナル応答性遺伝子発現

（米国学士院）

図1　内分泌かく乱仮説と生物学的蓋然性

して取り組むことになった。その申し合わせの1つとして、WHOは内分泌かく乱問題に関する世界的なアセスメント、グローバルアセスメントの編纂を20人ほどの編集委員をもって、3年計画で開始した。編集委員会では個々の事象を1つ1つ検討し、2002年、それまでその存在の如何についてもはっきりしていなかった内分泌かく乱現象に対し、最終的に、内分泌かく乱物質問題がすでに存在する概知の事象であろうと結論づけ、出版物として刊行した。

この時のまとめは4点あり、1)身体が形成されていく過程での曝露が、刺激に対する応答機能を恒久的に変化させてしまう可能性をもつこと、2)成熟した動物への曝露は、ホメオスタシス(恒常性)に基づいた応答により、顕著な影響を示さないかもしれないこと、3)発育段階の違いや季節変動などで同じホルモン様の影響が異なった結果を呈する可能性のあること、そして、4)内分泌系の異なった要素間でのクロストークにより予想外の影響を生ずる可能性のあることなどを挙げた。そして何より、内分泌かく乱化学物質問題は仮説の問題ではなく、すでに存在する既知のことがらであること、従って何らかの対応が必要なことを結論したことがその後に与えた影響には顕著なものがある。

グローバルアセスメントでは、内分泌かく乱化学物質が、成獣には影響を起こしにくいようであること、しかし、胎生期と新生児期の性成熟過程にあたる形態形成期では不可逆的影響を及ぼす可能性がある、といった点を強調した。この指摘により欧州機構や各国の取り組みが本格化した。昨年末のヘルシンキ会議は、さらに5年経って欧州機構などのこの問題に関する研究支援が本格的に軌道に乗った中で行われ、多くの新しい有用な研究情報が紹介された。会議最終日、ダイオキシン受容体研究で知られるジューコ・ツオミストが挨拶に立ち、野生生物の深刻な実態に比較した時のヒトのリスクを次のようにまとめた。「多くの内分泌かく乱物質は、経口的に摂

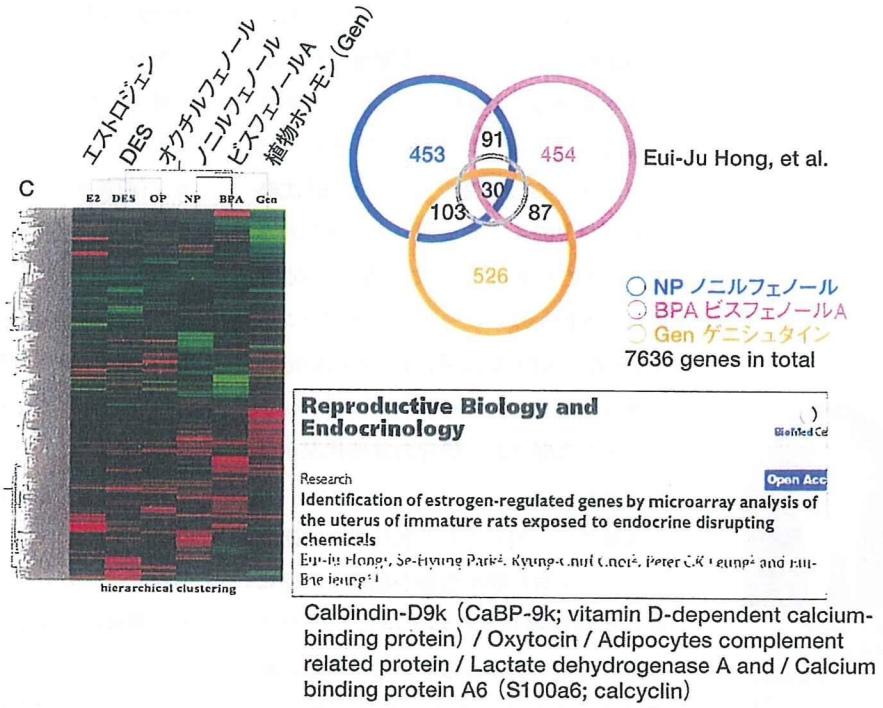

図2　遺伝子発現で見た内分泌かく乱化学物質の性質

左のキルト模様のようなグラフは、生体がどう反応しているのかを遺伝子の反応パターンで示している。左図のエストロジェン、DES、オクチルフェノールなどは、いずれも女性ホルモン様の作用をもつとされている。しかし、グラフに明らかなとおり、横一直線に共通した反応は見られない。右のバイグラフも同様であり、ノニルフェノール、ビスフェノールA、ゲニシュタインの3つの化学物質で共通に発現する遺伝子は30個検出されるのみである。つまり、内分泌かく乱化学物質といっても、ヒトに共通に影響を与える目印になる遺伝子は見られず、したがって、十把一絡げにその特徴を判断するわけには行かない、ということがわかる。

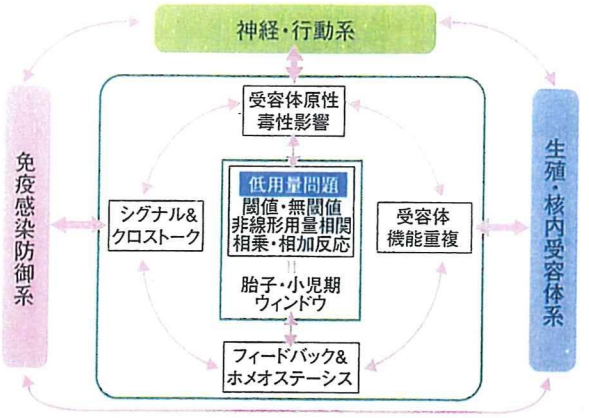

図3　分泌かく乱化学物質の高次生命系への影響（模式図）
神経・行動系、免疫感染防御系、そして生殖・核内受容体系、の3系統に重点を置いた研究が進められている。これらの臓器では、ホルモン受容体が普段から発現していて、共通のさまざまな因子の発現が観察される。それぞれが長期の記憶装置をもっていることも特徴である。

取されるであろう。しかし、ヒトの摂取する食物と水とは、その衛生管理が整っており、そこで、ヒトへの曝露は、事実上認められない」というものである。おそらく、そうした紙一重の状態が、ヒトへのリスクを押さえているというのが実態なのだろう。

新しくわかったこと、今後必要性な研究

以上がこれまでの概略であるが、初期、危惧されていた事柄などを通覧すると、人々の身のまわりにはホルモン様物質がたくさんあり、その中では生体ホルモンでさえ、本来、ある程度生体に有害な性質をもつ。雌雄対偶動物の身体の中ではこれが"漏れ出さないよう"緻密な自己防護システムが備わっていること、あるいは内分泌かく乱化学物質とよばれるものに、物質としての共通作用の乏しいこと（図2）、さらには、そうした化学物質の複合作用の有無など、多くの事柄で、多分に整理されないまま、机上の論議が行われてきた感が否めず、実験生物学の立場から見ると、充分に的を射た議論が行われてこなかったように思われる。

他方、筆者らは、内分泌かく乱化学物質の生体影響研究では、ホルモン受容体が普段から発現していて、いろいろな共通の補助因子の発現が観察され、それぞれが長期の記憶装置をもっていること、神経・行動系、免疫・感染防御系、そして生殖・核内受容体系などの諸系統に注目することの重要性を、これまでにも啓蒙書[1]を出版したりして強調してきた（図3）。幸いなことに、この考えはかなり妥当な判断だったようで、一連の研究からは、0.01～0.2mg／kg／dayという無作用量以下の低用量のビスフェノールAに、神経・行動異常を引き起こす作用が見出されており[2]、諸分野で、注目すべき新たな知見と今後の研究の展望が明らかに成りつつある。ここでは、特記すべき点のみ、かいつまんで紹介する。

1．用量－反応曲線と低用量への外挿性

毒性学による安全性の試験では、高用量の反応から直線回帰をして低い用量での反応性を予測することが多い。したがって、低用量での作用が明らかになりつつある内分泌かく乱化学物質の作用曲線について、無作用量以下の低用量域で外挿表徴型と異なった反応がないかどうか

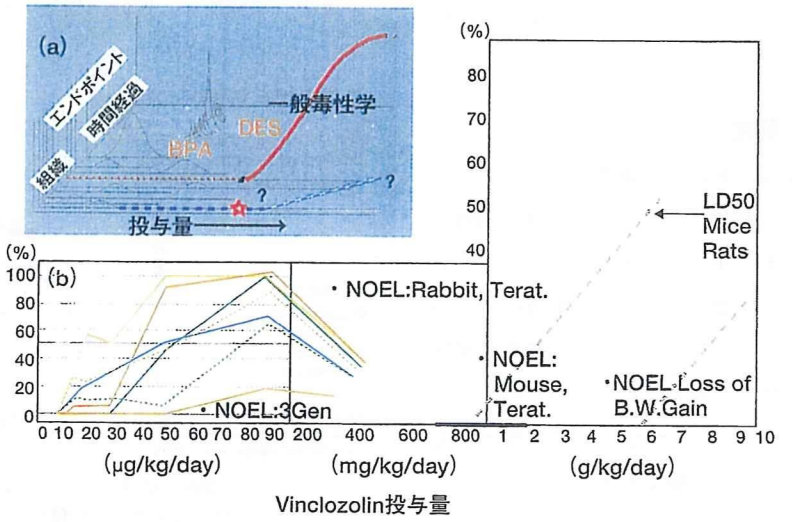

図4　低用量域の変化と稀少特性
既存のデータを整理すると、従来は、無作用量、無毒性量と定めていた用量より低い濃度で、さまざまな影響が観察されることが報告されている。
（b：米国の国立環境影響研究所NIEERLのEarl Gray博士による）

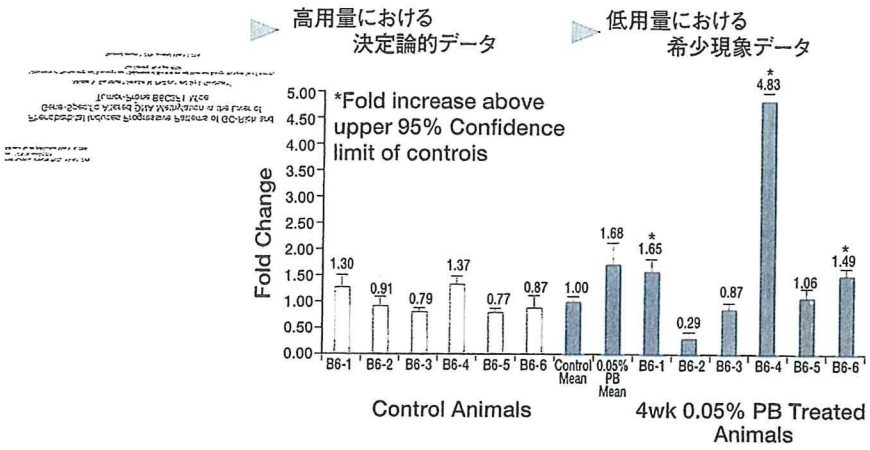

図5　低用量域の変化と稀少特性

低用量域で種々の試験法に沿って実験をすると、純系動物を用いた実験でも、変動幅の広い結果得られることがある。図は、フェノバルビタールによるメチル化部位の形成確率を、ネズミ一匹毎に検出したもの。対照群と異なり、個体毎の値が広く分布している。内分泌かく乱化学物質影響にもこうしたエピジェネティック特性が想定される。(ミシガン州立大学のJay Goodman教授による)

の如何については、早くから議論があった。そして実際に既存のデータを整理すると、従来無作用量とか、無毒性量と定めた用量より低い濃度でさまざまなデータが認められた。米国環境防護庁所轄の国立環境影響研究センターでは多年度計画を立てて検討に入っている[3] (図4)。

2. 低用量反応の問題点

メチル化は、たとえ純系動物でも確率論的に形成され、等質の結果が出ないことがわかってきた（図5)。こうした結果に対して平均値を取ると、ばらつきは背景データに隠れてしまうので、“プロクラステスのベッド”*で知られる通り、禁忌とされる。

*プロクラテスは、一面に宝石を散りばめた黄金のベッドの寸法よりも客の寸法が短いと、ベッドの寸法に合うよう4人の力持ちの大男に引き延ばさせたり、ベッドよりも長いと頭や足を切り落とさせたという。

3. 発がん蓋然性の問題

発がん性との関係では、発がんの蓋然性、つまり、これらの物質によってがんが起こりやすそうな体内環境が形成される可能性があるのかどうかという点である。女性ホルモンとダイオキシン類の1つが、正常のmycという遺伝子と協同して、テロメラーゼという、細胞を無限増殖へ導く遺伝子の活性を引き上げた、という報告がある[4]。こうした変化は、がん化につながる可能性があるため、早急に検証することが必要である。

4. 思春期早発の蓋然性と加齢影響

内分泌かく乱化学物質の性質の1つとして、思春期を早く発来させ、早期の老化を引き起こすなどといった点に危惧があった。図6に示したように、ビスフェノールAの効果では、投与した動物の寿命曲線が、グラフの白○印の対象に較べて、死亡が早期化し、傾きも急峻になる傾向があることがわかる[5]。もしこの寿命曲線が正しいとすると、これまで見てきた生殖リスク評価センター(CERHR)の判断とはまったく違った結果になるわけであり、これについても、よく調べる必要がある。

5. 内分泌器官の拡張

さて、次に注目すべき点は、結論から述べると、これまで内分泌器官と一括して述べたが、よく調べてみると、肝臓や脂肪細胞など、従来必ずしも内分泌器官と考えてこなかった臓器が、内分泌器官の役割をしていると、い

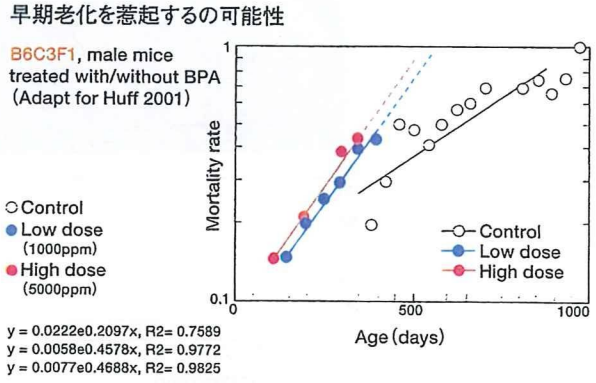

図6　ビスフェノールAによる
エピジェネティック発がんと促進老化

内分泌かく乱化学物質の性質の1つとして、思春期の早発や早期老化が危惧されてきた。ビスフェノールAを投与した動物の寿命曲線は、白○印の対象に較べて、死亡が早期化し、傾きも急峻になる傾向が見られる。ビスフェノールAは、エピジェネティック発がんの促進が見られるようである。(文献5より引用改変)

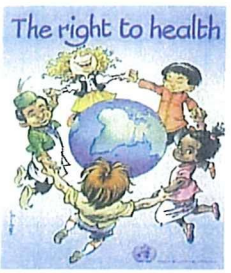

図7　低用量問題と胎生期ウィンドウ

内分泌かく乱化学物質は、形態形成期の臨界投与期に障害を引き起こすのでこれをウィンドウ効果とよんでいる。臨界投与量(0.003mg/kg)のDESという物質で尿道下裂が引き起こされる時期も、生後7日の新生児期に限局している(基生研、井口泰泉教授による)。世界保健機構が子どもの健康に力をいれる所以である。

えなくもないということである。たとえば、ノニルフェノールという物質は、通常の方法で見るとごく弱い女性ホルモン様の作用をもっているのであるが、肝臓に注目すると、女性ホルモンよりも、ずっと強い活性をもっていることが、基礎生物学研究所・井口泰泉教授らの研究でわかった。すると、肝臓は、内分泌器官なのだろうかという疑問がもたれる。

6. 内分泌の概念の拡張

続いて、内分泌器官の概念の拡張にかかわる事柄である。異物受容体とよんでいるダイオキシン受容体は、エストロジェンが存在しない状態では、P300と名づけているタンパク分子の助けで転写活性化を担い、なんと、女性ホルモン様の作用をもつことがわかった。しかも、エストロジェンがある時は、この分子は、これと反対にUbiquitin ligaseとよばれる複合体を形成し、エストロジェン受容体を壊して、抗女性ホルモン様の役割を発揮することもわかってきた。このように、ホルモン受容体でもない、こうした生体内分子としての異物受容体が、ホルモン様の作用を発揮するということは、内分泌かく乱問題の分子的基盤が、大きく拡大していくことを示している。これは非常に大きな驚くべき問題といわねばならない。しばらくして、日本発のこの東京大学分子細胞生物学研究所・加藤茂明教授のグループによる研究は、Natureに紹介された[6]。

おわりに

最後に一言、"子どもの問題"に触れて、本稿を終了したい(図7)。

低用量問題は、胎生期ウィンドウに密接に関連していることを前述した。これは神経・行動学的不可逆性にも関連している。したがって、内分泌かく乱化学物質研究は"子ども"の毒性学研究に重なり合うところが大きい[7]。近年、"子どもは小さな大人ではない"、ということが指摘されるようになった。WHOはこの点を重視して事業目標の重点に据えている。この概念が広く認識されることの意義には疑義がない。そうした前進にもかかわらず蛇足として指摘したい点は、この"子どもの特性"が量的な差異ではなく、質的な差異に基づいている、ということである。しばしば、"子どもの反応性"が脆弱で可塑的であるから安全係数を負荷するといった試みがなされている(たとえば米国EPAでは、一定の判断の下に5を除する)。筆者は、これはまさに"子どもを小さな大人"と扱ったもの以外の何物でもないことを指弾している。つまり"子ども"には、数値で大人と比較しきれない、本質的に大人と異なった事柄がある、という蓋然性は、ここでは考慮に入れられていないに等しい。この点を正しく認識するためには、成長過程の"子ども"についてのさらに深い研究が必要である。

[参考文献]

1) 井上達, 井口泰泉：生体統御システムと内分泌かく乱, シュプリンガー・フェアラーク東京, pp.324, 2007.
2) Kubo K, et al.：Neurosci. Res., 45: 345-356, 2003.
3) Office of Research and Development, US-EPA: Multi-year plan (FY2000-2012) for endocrine disruptors. http://www.epa.gov/nerl/goals/ecosystem/edc.html
4) Sarkar P, et al.：Intn'l. J. Oncol., 28: 43-51, 2006.
5) Huff J：Odontology, 89: 12-20, 2001.
6) Ohtake F, et al.：Nature, 423: 545-550, 2003.
7) http://cfpub.epa.gov/ncer_abstracts/index.cfm/fuseaction/display.researchCategory/rc_id/842

Environ. Sci. Technol. 2007, 41, 3775–3780

Aryl Hydrocarbon Receptor Plays a Significant Role in Mediating Airborne Particulate-Induced Carcinogenesis in Mice

YUTAKA MATSUMOTO,*,†,§ FUMIO IDE,‡ REIKO KISHI,† TOMOKO AKUTAGAWA,§ SHIGEKATSU SAKAI,§ MASAFUMI NAKAMURA,∥ TOSHITAKA ISHIKAWA,⊥ YOSHIAKI FUJII-KURIYAMA,# AND YOKO NAKATSURU⊥

Department of Public Health, Graduate School of Medicine, Hokkaido University, Sapporo, Japan, Department of Oral Pathology, Meikai University School of Dentistry, Saitama, Japan, Department of Environmental Protection, Hokkaido Research Institute of Environmental Sciences, Sapporo, Japan, Hiyoshi Corporation, Shiga, Japan, Department of Pathology, Faculty of Medicine, University of Tokyo, Tokyo, Japan, and TARA Center, University of Tsukuba, Tsukuba, Japan

Urban particulate air pollution is associated with an increased incidence of cancers, and especially lung cancer. Organic extracts of airborne particulate matter (APM) cause cancer in mice, and PAHs adsorbed to APM are associated with particle-induced carcinogenesis. PAHs are agonists for AhR and are predominantly responsible for lung cancer through induction of highly carcinogenic metabolites. PAH metabolization requires CYP1A1 induction through activation of AhR, and therefore we hypothesized that carcinogenesis due to PAHs in APM would be reduced in AhR−/− mice. To examine this hypothesis, we performed a long-term continuous-application study of carcinogenesis in AhR−/− mice using airborne particulate extract (APE) of APM collected in Sapporo. Tumor development (squamous cell carcinoma) occurred in 8 of 17 AhR+/+ mice (47%), but no tumors were found in AhR−/− mice, and CYP1A1 was induced in AhR+/+ mice but not in AhR−/− mice. These results demonstrate that AhR plays a significant role in APE-induced carcinogenesis in AhR+/+ mice and CYP1A1 activation of carcinogenic PAHs is also of importance. Therefore, measurement of CYP1A1 induction in vitro may be useful for assessment of APM-induced carcinogenesis in humans. We also show that PAH-like compounds are major contributors to AhR-mediated carcinogenesis, whereas TCDD and related compounds make a smaller contribution.

Introduction

Urban air particulate matter (APM) are mutagenic in short-term genetic bioassays (*1*, *2*), and many exhibit carcinogenic activity in vitro and in vivo (*3*). Epidemiological studies show that urban particulate air pollution is a risk factor for lung cancer (*4*, *5*). However, the biological mechanisms underlying APM carcinogenicity remain unknown.

Among the numerous genotoxic and carcinogenic compounds adsorbed onto urban APM, polycyclic aromatic hydrocarbons (PAHs) are the most prominent because of their known carcinogenic and/or mutagenic properties (*6*, *7*). The carcinogenicity of PAHs occurs through metabolic activation by cytochrome P450 and epoxide hydrolase, which results in formation of highly carcinogenic diol-epoxide metabolites that form DNA adducts that initiate the carcinogenic process (*8*).

Among the cytochrome P450s, CYP1A1 and CYP1B1 have important roles in metabolic activation of carcinogenic PAHs (*9*). Induction of drug-metabolizing enzymes including CYP1A1 and CYP1B1 by PAHs and other environmental contaminants is mediated by a ubiquitous intracellular receptor called the aryl hydrocarbon receptor (AhR) (*10*). AhR is a ligand-activated transcription factor that occurs in many cells and tissues and mediates PAH-induced toxicity, teratogenicity, and carcinogenicity (*11*). Increased expression of AhR occurs in human lung carcinoma compared to normal human lung tissues (*12*). APM extracts induce CYP1A1 and CYP1B1 in the human lung-derived cell line CL5 (*13*) and show significant AhR-mediated activity in vitro in ethoxyresorufin-*O*-deethylase (EROD) induction and in an AhR luciferase reporter system (*14*).

Previously, we have shown that the skin carcinogenicity of BaP, a prototypical PAH, is lost in AhR-deficient (AhR−/−) mice, suggesting that AhR-mediated induction of CYP1A1 is important in BaP-induced skin carcinogenesis in mouse (*15*). We also reported that the skin carcinogenicity of dibenzo-[*a*,*l*]pyrene (DB[*a*,*l*]P), a powerful carcinogenic PAH (*16*), was dramatically suppressed in AhR−/− mice, suggesting that the AhR-induced CYP1A1 expression may correlate with susceptibility to DB[*a*,*l*]P carcinogenesis (*17*). These findings imply that AhR-mediated induction of P450s including CYP1A1 is important in activation of PAHs in mouse carcinogenesis.

For evaluating health risks, an understanding of the role of AhR in carcinogenesis caused by environmental mixtures is of importance since people are exposed to such mixtures in daily life. To date, there is no direct proof that AhR plays a significant role in vivo as a mediator of carcinogenesis of environmental mixtures, including APM. However, 2,3,7,8-tetrachlorodibenzo-*p*-dioxin (TCDD) and related compounds as well as PAHs can bind to AhR to elicit induction of P450s, and urban APM is a complex mixture of substances such as PAHs, TCDD, and related compounds. Therefore, the immunotoxic and carcinogenic reactions elicited by PAHs and TCDD in APM may be mediated by AhR.

The main objective of this study was to examine whether AhR signaling has a net potentiating effect on APM carcinogenicity in mice. Skin tumorgenesis was investigated by long-term treatment with an APM extract (airborne particulate extract; APE) collected by hi-volume samplers, through topical application to the skin of wild type AhR+/+ and AhR−/− mice. A second aim was to evaluate the AhR-mediated biological activity of APE and to differentiate the effect on this activity of PAHs from that of TCDD and related compounds. For this purpose, AhR-mediated activity was determined with crude and cleaned APE, using a reporter-gene assay based on chemically activated luciferase expression (the CALUX assay).

* Corresponding author phone/fax: +81-11-643-0093; e-mail: yt-matsu@zpost.plala.or.jp
† Hokkaido University.
‡ Meikai University School of Dentistry.
§ Hokkaido Research Institute of Environmental Sciences.
∥ Hiyoshi Corporation.
⊥ University of Tokyo.
University of Tsukuba.

10.1021/es062793g CCC: $37.00 © 2007 American Chemical Society
Published on Web 04/17/2007

Materials and Methods

Air Particulate Samples. APM samples were collected on the roof of the Hokkaido Research Institute of Environmental Sciences, which is situated in a residential area about 2 km from the center of Sapporo and entirely surrounded by fields and grounds and not affected directly by vehicle exhaust PM. APM was collected on glass or tissue quartz-filters using high-volume samplers at a rate of 80 m^3/h during the cold season (October–March) from 1973 to 1986. Exposed filters were replaced with new filters daily. A total of 910 24-h filter samples were obtained by filtering 1 770 000 m^3 of air. After weighing the filter samples, they were placed in plastic sacks, vacuum sealed, and maintained in the refrigerator room at a constant −20 °C. The extraction procedure was conducted immediately before the chemical analysis, in vitro bioassay, and the beginning of the animal experimentation (April 2001). To ensure storage of filter samples was suitable, comparative studies were made for the 19-year period. During the storage of the filter samples from 1988 to 2007, no significant changes in mutagenic activity and PAHs concentration were detected. Thus, we presume that there was little or no degradation of the stored samples over time (1973–2001).

Extraction of Organic Matter. Organic material was extracted from the filter samples by ultrasonication using dichloromethane. After filtration through paper to remove undissolved matter, the APE samples were combined. A portion was dried, dissolved in hexane or dimethyl sulfoxide, and used for analysis of PAHs and TCDD and related compounds or for mutagenicity testing and the CALUX assay, respectively. Another portion of APE was used in a skin-painting experiment.

Chemical Analysis and Mutagenicity Test of APE. Sixteen PAHs including six carcinogenic PAHs according to IARC evaluation in APE (Table 1) were analyzed on an Agilent 6890 gas chromatograph (GC) with a 5973 mass spectrometer (MSD) using selected ion monitoring. A DB-5 MS column (J&W Scientific; 30 m × 0.25 mm i.d.; film thickness, 0.25 μm) was used to separate the PAHs. Dioxin-like compounds (17 polychlorinated dibenzo-*p*-dioxins (PCDDs) and dibenzo-*p*-furans (PCDFs)) and 12 PCBs were analyzed by high-resolution gas chromatography-high-resolution mass spectrometry (HRGC-HRMS). A toxicity equivalent (Eq) value for each compound was calculated using the WHO-toxicity equivalent factor (TEF). The total Eq concentration based on HRGC-HRMS analysis (Chemical TCDDEq) for APE was yielded by summation of the calculated Eq concentration for each dioxin-like compound. Mutagenicity of APE was examined by preincubation in the Ames mutagenicity test (*18*) using *Salmonella typhimurium* TA98 and TA100 with (+S9 mix) and without metabolic activation (−S9 mix).

Determination of AhR Mediated Activity of APE. AhR-mediated activity of APE was determined by the CALUX assay, which is based on a genetically engineered rat H4IIE hepatoma cell line with an AhR-controlled firefly luciferase reporter gene construct for detection of CYP1A1-inducing compounds in APE. The assays were performed in 96-well plates as described previously (*19*). Briefly, 24 h after seeding the cells were dosed with crude APE or cleaned APE. Using a sulfuric acid silica column, the APE was cleaned by removing PAHs and PAH-related compounds (PAH-like compounds), including PAHs, nitroarenes, aza-arenes, aminoarenes, methyl-
arenes, etc. The exposure time was either 3 h to measure most compounds (especially PAHs) or 24 h to measure TCDD and related compounds, which are resistant to biotransformation in the cells. The final results are expressed as toxicity equivalents (Eq) in the CALUX assay for BaP (CALUX BaPEq) or TCDD (CALUX TCDDEq), based on the CALUX assay concentration–response curve of BaP or TCDD.

Detection of CYP1A1 by RT-PCR. APE (6.4 mg) was applied to the shaved back of mice once a week for 4 weeks. Six days after the last application, aliquots of RNA (1 μg) were extracted from the dorsal skin of control and APE-treated mice of the two genotypes, and the expression of CYP1A1 mRNA was determined by RT-PCR.

Preparation of Sample Extracts for skin Painting. The mutagenic activities in TA100 with S9 mix per unit of APE and BaP were 4840 and 310 000 revertants/mg, respectively. The amount of extract equivalent to mutagenicity of 1 mg of BaP in the Ames assay was 64 mg (310 000 ÷ 4840 = 64) of APE. Extract for skin painting was adjusted to a concentration equivalent to the mutagenic toxicity equivalent of BaP (M BaPEq) 100 μg (= APE 6.4 mg)/200 μL of acetone.

Animals Procedures. AhR−/− mice were developed by Mimura et al. (*20*). AhR+/+ (n = 17) and AhR−/− (n = 15) female mice aged 6–8 weeks old were used in the study. All mice were genotyped by PCR screening of DNA from the tip (*15, 20*). The animals were housed in clean racks in a filtered-air environment under controlled conditions of temperature (22 ± 1°C), relative humidity (50 ± 5%), and a 12-h light-dark cycle. Sterilized diets and water were available ad libitum throughout the study.

Treatment and Tumor Induction. The dorsal skin of AhR+/+ and AhR−/− mice was shaved 2 days before treatment. Acetone suspensions of APE at 32 mg/mL (equivalent to 500 μg/mL M BaPEq) prepared from the combined APE were epicutaneously dropped onto the shaved backs in a volume of 200 μL. A single application of 200 μL containing 6.4 mg of APE is equivalent to 100 μg M BaPEq. This dose of APE was chosen with toxicity in mind and to obtain data for comparison with the results of the continuous application test (*15*), in which 200 μg of BaP was used once a week. After the application, the mice were restrained until the acetone had completely evaporated. Treatment was repeated continuously once a week until a skin tumor was detected. Animals were inspected weekly for tumor development, and the numbers of skin tumor lesions of larger than 2 mm were counted. The mice were sacrificed and dissected in the 58th week. The main organs were fixed in 10% neutral-buffered formalin, embedded in paraffin as tissue slices, and sectioned and stained with hematoxylin and eosin for microscopic histopathological evaluation.

Statistical Analysis. The statistical significance of the difference in tumor incidence between AhR+/+ and AhR−/− mice was evaluated by Student t-test. A p value of less than 0.05 was considered significant.

Results

PAH Concentrations in APE. Quantitative chemical analysis of APE showed the presence of many carcinogenic PAHs, including BaP, dibenzo[*a,h*]anthracene (DahA), and indeno-[1,2,3-*cd*]pyrene (IND) (Table 1). Measured PAH concentrations were corrected for biological activity and expressed as BaP toxicity equivalent (BaPEq) concentration. The BaPEq concentration for each PAH was calculated by multiplying the PAH concentration by the corresponding TEF (*21*), using the TEFs given by Nisbet and LaGoy (*22*).

The BaPEq concentration and the relative contribution to carcinogenic activity of each PAH, expressed as a percentage of the total BaPEq concentration of the mixture, and the measured air concentration of each PAH are given in Table 1. Benzo[*b*+*j*]fluoranthene (BbjF) had the highest measured air concentration, followed by chrysene (Chr), benzo[*ghi*]-perylene (BghiP), IND, BaP, and BaA. A total BaPEq concentration of 10.2 ng/m^3 was calculated for APE (Table 1), and the BaPEq concentration of 5.6 ng/m^3 for BaP accounted for 55% of the total; therefore, BaP contributed most to the total calculated BaPEq concentration, in agreement with literature data (*23, 24*).

TABLE 1. Measured and TEF[a]-Adjusted (BaPEq) PAH Concentrations in APE

compound (abbreviation)	TEF[a]	measured concentration ng/m³, air	measured concentration (ng/mg, APE)	BaPEq concentration ng/m³, air	BaPEq concentration (ng/mg, APE)	rel contribution in BaPEq (%)
naphthalene (Naph)	0.001	0.23	(25)	0.0002	(0.025)	0.0
acenaphthylene (Aceny)	0.001	0.11	(12)	0.0001	(0.012)	0.0
fluorene (Flu)	0.001	0.13	(14)	0.0001	(0.014)	0.0
phenanthrene (Phen)	0.001	1.6	(173)	0.0016	(0.173)	0.0
anthracene (Ant)	0.01	0.38	(41)	0.0038	(0.41)	0.0
fluoranthene (Fluor)	0.001	4.2	(453)	0.0042	(0.45)	0.0
pyrene (Pyr)	0.001	4.6	(496)	0.0046	(0.50)	0.0
benzo[*a*]anthracene (BaA)[b]	0.1	5.5	(593)	0.55	(59)	5.4
chrycene (Chr)	0.01	9.1	(982)	0.091	(9.8)	0.9
benzo[*b*+*j*]fluoranthene (BjbF)[b]	0.1	11	(1187)	1.1	(119)	10.8
benzo[*k*]fluoranthene (BkF)[b]	0.1	4.6	(496)	0.46	(50)	4.5
benzo[*a*]pyrene (BaP)[b]	1	5.6	(604)	5.6	(604)	54.8
indeno[1,2,3-*cd*]pyrene (IND)[b]	0.1	6.2	(669)	0.62	(67)	6.1
dibenzo[*a*,*h*]anthracene (DahA)[b]	1	1.7	(183)	1.7	(183)	16.6
benzo[*ghi*]perylene (BghiP)	0.01	8.7	(939)	0.087	(9.4)	0.9
total				10.2	(1103.0)	100

[a] Data from ref *22*. [b] Probably or possibly carcinogenic to humans according to IARC evaluation.

TABLE 2. CALUX BaPEq, CALUX TCDDEq, and Chemical TCDDEq Concentrations in Crude or Cleaned APE

	CALUX BaPEq[a] ng/m³, air (ng/mg, APE)	CALUX TCDDEq[b] pg/m³, air (ng/mg, APE)	chemical TCDDEq[c] pg-TEQ/m³, air (pg-TEQ/mg, APE)	
crude APE	979 (105634)	21 (2266)		
cleaned APE	7.87 (849)	0.613 (66)		
				0.13 (14)
			PCDDs TEQ	0.036 (3.9)
			PCDFs TEQ	0.091 (9.8)
			Co-PCBs TEQ	0.0072 (0.78)

[a] CALUX BaPEq : BaP equivalent based on CALUX assay using a BaP standard curve. [b] CALUX TCDDEq : TCDD equivalent based on CALUX assay using a TCDD standard curve. [c] Chemical TCDDEq :TCDD equivalent based on HRGC-HRMS analysis.

Mutagenic Activity of APE. The TA100 strain was more sensitive to the mutagens in APE than the TA98 strain, both with and without metabolic activation. Addition of S9 produced an increase in mutagenic response in both strains, which indicates the presence of promutagens in APE (Data are not shown.).

AhR-Mediated Activity (CALUX Assay) and TCDD Concentration in APE. Luciferase expression induced by crude and cleaned APE was transformed into BaP or TCDD equivalent concentration using a BaP or TCDD standard curve based on response in the CALUX assay after a 3-h or 24-h exposure time. These data (CALUX BaPEq, CALUX TCDDEq) and the results of HRGC-HRMS analysis of TCDD and related compounds in cleaned APE (Chemical TCDDEq) are shown in Table 2. The CALUX BaPEq concentration of crude APE was 979 ng/m³ air, or 105634 ng/mg APE, and the measured BaP concentration (5.6 ng/m³) (Table 1) accounted for only 0.57% of CALUX BaPEq. The CALUX BaPEq of cleaned APE (7.87 ng/m³) accounted for only 0.80% of CALUX BaPEq for crude APE, suggesting that most of the CALUX BaPEq for crude APE was derived from PAH-like compounds in APE. Therefore, the small amount of CALUX BaPEq derived from TCDD and related compounds in cleaned APE could be ignored. Similarly, CALUX TCDDEq for cleaned APE (0.613 pg/m³) accounted for only 2.9% of CALUX TCDDEq for crude APE, showing that the contribution of TCDD and related compounds to CALUX TCDDEq for crude APE was very small. The concentration of TCDD and related compounds (Chemical TCDDEq) in the HRGC-HRMS analysis of cleaned APE was 0.13 pg/m³, and the relative rate of luciferase induction of TCDD for BaP (=1) after a 3-h exposure was 3.85×10^4. Based on these numbers, it was calculated that 0.13 pg/m³ of Chemical TCDDEq would be equivalent to 5.01 pg/m³ of CALUX BaPEq and that the contribution of this value to CALUX BaPEq for crude APE was as low as 0.51%. The contribution of 0.13 pg/m³ of Chemical TCDDEq to CALUX TCDDEq for crude APE was also low (0.62%).

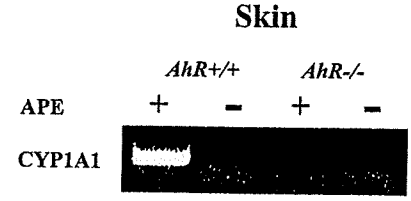

FIGURE 1. CYP1A1 gene expression in the skin of AhR+/+ and AhR−/− mice with and without APE treatment.

Induction of CYP1A1 by APE. Expression of CYP1A1 in the skin of AhR+/+ and AhR−/− mice was investigated using RT-PCR. Following APE treatment, CYP1A1 was induced in AhR+/+ mice but not in AhR−/− mice. No induction of CYP1A1 was apparent without APE treatment, regardless of the genotype (Figure 1). Therefore, the results show that APE induces CYP1A1 through an AhR-dependent pathway.

Tumor Incidence in Mice. APE suspended in acetone was continuously applied once weekly to the dorsal skin of 17 female AhR+/+ mice and 15 female AhR−/− mice. No tumors and hypertrophic changes were observed by the naked eye in AhR−/− mice, whereas AhR+/+ mice showed gradual depilation and inflammatory changes in the skin. In AhR+/+ mice, the first subcutaneous tumor appeared 29 weeks after initiation of treatment, and tumors were present in 3 mice after 41 weeks and 5 mice after 49 weeks. After 58 weeks, 8 of the 17 mice (47%) had papillomatous tumors of larger than 2 mm. Of the 8 induced tumors, 6 were solitary, but multiple tumors occurred in two mice: one having two and one having three small papillomas. In tissue examination under a microscope, it was found that all of the 2-mm or larger tumors in AhR+/+ mice were squamous cell carci-

TABLE 3. Incidence of Skin Tumors Induced in Two Mouse Genotypes after Repeated Application of APE

	AhR genotype	
	+/+	−/−
no. of mice	17	15
squamous cell carcinoma	8	0
papilloma	0	0
keratocanthoma	0	0
total no. of tumor-bearing mice (%)	8 (47%)	0 (0%)

noma, which showed infiltrative growth into muscular tissues in parts of the whole tumor (histopathological image). In addition, erosion and bleeding, which were thought to be caused by extract toxicity, were observed in the anal region of a few AhR+/+ mice. In AhR−/− mice, no tumors developed in the experimental period of 58 weeks, giving a statistically significant difference in tumor incidence between AhR+/+ and AhR−/− mice (8/17 vs 0/15, $p < 0.01$; Table 3). The gross appearance of back skins in AhR+/+ and AhR−/− mice after 58 weeks following repeated application of APE is illustrated in Figure 2. No tumors were evident in internal organs, and there were no other remarkable side effects or observations.

Discussion

PAHs in APE are important environmental carcinogens that pass through the cell membrane and bind to AhR, leading to induction of drug-metabolizing enzymes such as CYP1A1. PAHs are metabolically activated by these enzymes and transformed to DNA-binding carcinogenic substances. Therefore, carcinogenesis caused by PAHs in APE should be decreased in AhR−/− mice, since transactivation of the drug-metabolizing enzymes will not occur. A study in AhR−/− mice showed that acute toxicity or teratogenicity of dioxin is AhR-dependent (*20, 25*), and our previous study of BaP in AhR−/− mice suggested that induction of CYP1A1 via AhR and metabolic activation of BaP by this enzyme are important in BaP carcinogenesis (*15*). Therefore, the current study was performed to examine the potential AhR dependence of carcinogenesis caused by APE derived from APM, an environmental mixture of compounds collected in Sapporo, in AhR+/+ and AhR−/− mice.

Tumor Incidence and CYP1A1 Expression in AhR+/+ Mice. APE treatment induced CYP1A1 gene expression in AhR+/+ mice and tumors were observed in 47% of these mice over 58 weeks. In contrast, CYP1A1 was not induced, and tumor formation was completely suppressed in AhR−/− mice. These results provide strong support for the hypothesis that the carcinogenic action of APE is mediated primarily by AhR. The primary route of metabolic activation of PAHs involves induction of CYP1A1 mediated by AhR (*10*), which leads to enhanced turnover of PAHs and increased production of highly carcinogenic metabolites. The expression of CYP1A1 in the skin of APE-treated AhR+/+ mice (Figure 1) is in agreement with our earlier study showing CYP1A1 gene expression induced by BaP (*15*). Therefore, it is likely that AhR plays an important role in conversion of APE into carcinogenic compounds through induction of CYP1A1. In the present study, Ahr −/− mice were resistant to APE-induced skin carcinogenesis as well as BaP. On the other hand, there has been a report indicating that Ahr −/− mice were not less susceptible to BaP induced adduct formation when BaP was administered orally (*26*). In addition, the toxicity of BaP is augmented in AhR nonresponsive (*27*) and CYP knockout mice (*28*). Further long-term carcinogenesis studies using oral administration are needed to address the paradoxical effect regarding carcinogenicity and genotoxicity.

Following APE application to skin, tumors occurred in 47% of AhR+/+ mice over about 14 months but not at all in AhR−/− mice, suggesting that APE causes AhR-dependent carcinogenesis. In an application test performed with BaP only, tumors developed in 94% of AhR+/+ mice in 6 months with administration of 200 μg of BaP per week (*15*), compared to 100 μg of APE M BaPEq in the current study. We note that the correlation between mutagenesis and carcinogenesis is complex (*29*), and use of the value of M BaPEq dose, instead of BaP dose, may not necessarily be appropriate; thus, care should be taken regarding interpretation of data using the applied amount of APE based on M BaPEq, as discussed below.

Contribution of PAHs to the Carcinogenic Effect. The contribution of BaP alone to the total BaPEq concentration of APE was 55% (Table 1). BaP is the most studied PAH compound and is thought to be representative of the 16 PAHs in the APE in this study; however, BaP is just one of at least 100 PAHs that have been identified in APM and just one of many carcinogenic compounds in the atmosphere. In our previous application test using only BaP, the applied amount was 200 μg. Since the 6.4 mg dose of APE per week in the current study contained only 3.87 μg BaP, the tumor incidence in the APE-treated AhR+/+ mice does not appear to be solely due to BaP in the mixture. The contribution of BaP to total carcinogenesis capacity is reported to be 6−7.4% and 2.4% for gasoline-powered vehicles (*30, 31*) and 1.4% for flue gas-condensed substances in coal-heating furnaces (*32*). Based on these data, the contribution of BaP to APE carcinogenesis is estimated to be about 5% or lower.

The contribution to the total carcinogenicity of the PAH fraction comprising compounds with 3, 4, or more rings has been estimated to be 84−91% and 81% for gasoline-engine exhaust (*30, 31*), and the PAH fraction seems to contribute predominantly to the total carcinogenicity of diesel exhaust (*33*) and hard-coal combustion flue gas condensate (*32*). The major sources of air pollution in Sapporo from 1973 to 1986 were gasoline-powered vehicles, diesel-powered vehicles, and coal firing for home heating, suggesting that most carcinogenesis caused by APE is due to PAHs from such pollution sources. However, the contribution of carcinogenic compounds in APM other than PAHs, such as nitroarenes (NO_2-PAHs), aza-arenes, and polycyclic aromatic compounds (*34*), should also be taken into account. Continuous application of gas condensed substances from home heating furnace to

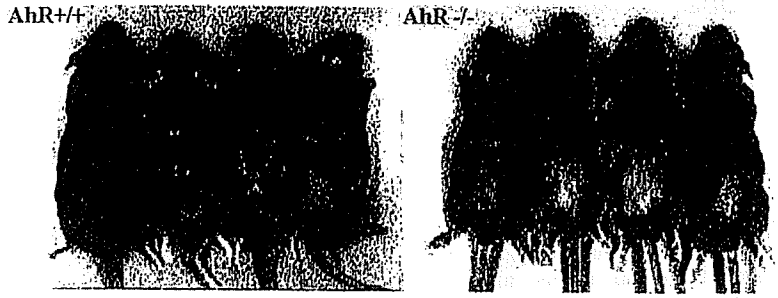

FIGURE 2. Gross appearance of skin tumors in AhR+/+ and AhR−/− mice after repeated application of APE.

the back of mice has shown that fractions including nitroarenes and aza-arenes account for only 4–7% of total carcinogenesis capacity (*35*). However, nitroarenes are an important subgroup of PAHs found in extracts from diesel and gasoline engine exhausts. 3-Nitrobenzanthrone (3-NBA) is an extremely potent mutagen and suspected human carcinogen that is one of several nitroarenes identified in urban PM. Recently, it has been reported that CYP1A1/2 could play an important role in the oxidative metabolism of 3-NBA and the main metabolite of 3-NBA, 3-aminobenzanthrone, to reactive DNA adducts, thereby enhancing their own genotoxic potential (*36, 37*). Thus, for accurate risk assessment of nitroarenes including 3-NBA, further studies on the carcinogenic effect after metabolic activation by P450s are required.

BaPEq Concentration. The carcinogenic potency of a PAH can be assessed based on its BaPEq concentration, and the total BaPEq concentration in mixtures is obtained from the sum of the BaPEq concentrations of components, assuming additive carcinogenic effects in the mixture. BaP had the highest contribution to the total calculated BaPEq concentration (55%), indicating the importance of BaP as a surrogate compound for PAHs mixtures in air; BaP contributions of 42–50% and 50–67% in urban air have also been reported (*23, 24*).

AhR Mediated Activity (CALUX BaPEq and CALUX TCDDEq). Evaluation of AhR-mediated activity of urban APM is important toxicologically for characterization of its carcinogenic potential. In the current study, AhR-mediated activity of APE was determined using the CALUX assay, for crude APE and cleaned APE, to differentiate the contribution to this activity of PAH-like compounds and TCDD and related compounds. A significant induction of AhR-mediated activity was observed for crude extract, expressed as CALUX BaPEq 979 ng/m^3 and CALUX TCDDEq 21.0 pg/m^3. The health consequences of these data are unknown, but this activity might contribute to adverse health effects of APM. The health risks of APM including PAH like compounds and dioxins will be assessed in further in vivo studies.

The CALUX assay response of crude APE may be due to both easily biodegradable and persistent AhR agonists, such as PAHs and TCDD, respectively. To test whether TCDD and related compounds contribute to the AhR-mediated activity of crude APE, cleaned APE was tested in 3-h and 24-h CALUX assays. A reduction in AhR-mediated activity due to depletion of PAH-like compounds in cleaned APE was observed for both CALUX BaPEq and CALUX TCDDEq, suggesting that PAH-like compounds are responsible for most AhR-mediated activity in crude APE. As PAHs, PAH-related compounds may be able to bind to and activate AhR. These compounds may include possible human and/or animals carcinogens. The Chemical TCDDEq concentration of 0.13 pg/m^3 indicates that TCDD and related compounds make relatively small contributions to this activity.

Finally, Revel et al. have demonstrated in an animal model that a natural AhR antagonist, resveratrol, inhibits BaP-induced CYP1A1 enzyme activity and subsequent formation of DNA adducts (*38*). Given the importance of AhR in APM-induced carcinogenesis, a competitive AhR inhibitor may provide a chemopreventive effect against development of cancer. Therefore, long-term exposure to APM in mice would be useful for evaluation of prevention of cancer by AhR antagonists.

In conclusion, our results show that APE induces carcinogenesis in AhR+/+ mice and provide the first direct evidence that AhR plays an essential role in APE-induced carcinogenesis. Our data also indicate that PAH-like compounds are significant contributors to AhR-mediated activity, whereas TCDD and related compounds make an almost negligible contribution.

Acknowledgments

This work was in part supported by a grant for Scientific Research on Special Areas from the Ministry of Education and Science of Japan and by a grant from the Smoking Research Foundation.

Literature Cited

(1) Matsumoto, Y.; Sakai, S.; Kato, T.; Nakajima, T.; Satoh, H. Long-Term Trends of Particulate Mutagenic Activity in the Atmosphere Sapporo. 1. Determination of Mutagenic Activity by the Conventional Tester Strains TA98 and TA100 during an 18-Year Period (1974–1992). *Environ. Sci. Technol.* **1998**, *32*, 2665–2671.

(2) Zhao, X.; Wan, Z.; Chen, G.; Zhu, H.; Jiang, S.; Yao, J. Genotoxic activity of extractable organic matter from urban airborne particles in Shanghai, China. *Mutat. Res.* **2002**, *514*, 177–192.

(3) Seemayer, N. H.; Hornberg, C. Malignant transformation of Syrian hamster kidney cells in vitro by interaction of airborne particulates and simian virus (SV-) 40. *Toxicol. Lett.* **1998**, *96/97*, 231–238.

(4) Hemminki, K.; Pershagen, G. Cancer Risk of Air Pollution: Epidemiological Evidence. *Environ. Health Perspect.* **1994**, *102*(Suppl 4), 187–192.

(5) Pope, C. A.; Burnett, R. T.; Thun, M. J.; Calle, E. E.; Krewski, D.; Ito, K.; Thurston, G. D. Lung Cancer, Cardiopulmonary Mortality, and Long-term Exposure to Fine Particulate Air Pollution. *JAMA* **2002**, *287*, 1132–1141.

(6) Lewtas, J. *Experimental Evidence for the Carcinogenicity of Air Pollutants. Air Pollution and Human Cancer*; Springer-Verlag: Berlin, 1990; pp 49–61.

(7) Pelkonen, O.; Nebert, D. W. Metabolism of polycyclic aromatic hydrocarbons: etiologic role in carcinogenesis. *Pharmacol. Rev.* **1982**, *34*, 189–222.

(8) Szeliga, J.; Dipple, A. DNA adduct formation by polycyclic aromatic hydrocarbon dihydrodiol epoxides. *Chem. Res. Toxicol.* **1998**, *11*, 1–11.

(9) Shimada, T.; Oda, Y.; Gillam, E. M. J.; Guengerich, F. P.; Inoue, K. Metabolic activation of polycyclic aromatic hydrocarbons and other procarcinogens by cytochromes P450 1A1 and P450 1B1 allelic variants and other human cytochromes P450 in *Salmonella typhymurium* NM2009. *Drug Metab. Dispos.* **2001**, *29*, 1176–1182.

(10) Shimada, T.; Sugie, A.; Shindo, M.; Nakajima, T.; Azuma, E.; Hashimoto, M.; Inoue, K. Tissue-specific induction of cytochromes P450 1A1 and 1B1 by polycyclic aromatic hydrocarbons and polychlorinated biphenyls in engineered C57BL/6J mice of arylhydrocarbon receptor gene. *Toxicol. Appl. Pharmacol.* **2002**, *187*, 1–10.

(11) Nebert, D. W,; Roe, A. L,; Dieter, M. Z.; Solis, W. A.; Yang, S. Y.; Dalton, T. P. Role of the aromatic hydrocarbon receptor and *[Ah]* gene battery in the oxidative stress response, cell cycle control, and apoptosis. Biochem. *Pharmacology* **2000**, *59*, 65–85.

(12) Lin, P.; Chang, H.; Tsai, WT.; Wu, MH.; Liao, YS.; Chen, JT.; Su, JM. Overexpression of Aryl Hydrocarbon Receptor in Human Lung Carcinomas. *Toxicol. Pathol.* **2003**, *31*, 22–30.

(13) Wang, H. W.; Chen, T. L.; Yang, P. C.; Ma, Y. C.; Yu, C. C.; Ueng, T. H. Induction of cytochromes P450 1A1 and 1B1 in human lung adenocarcinoma CL5 cells by frying-meat emission particulate. *Food Chem. Toxicol.* **2002**, *40*, 653–661.

(14) Arrieta, D. E.; Ontiveros, C. C.; Li, W-W.; Garcia, J. H.; Denison, M. S.; McDonald, J. D.; Burchiel, S. W.; Washburn, B. S. Aryl Hydrocarbon Receptor-Mediated Activity of Particulate Organic Matter from the Paso del Norte Airshed along the U.S.-Mexico Border. *Environ. Health Perspect.* **2003**, *111*, 1299–1305.

(15) Shimizu, Y.; Nakatsuru, Y.; Ichinose, M.; Takahashi, Y.; Kume, H.; Mimura, J.; Fujii-Kuriyama, Y.; Ishikawa, T. Benzo[a]pyrene carcinogenicity is lost in mice lacking the aryl hydrocarbon receptor. *Proc. Natl. Acad. Sci. U.S.A.* **2000**, *97*, 779–782.

(16) Pufulete, M.; Battershill, J.; Boobis, A.; Fielder, R. Approaches to carcinogenic risk assessment for polycyclic aromatic hydrocarbons: a UK perspective. *Regul. Toxicol. Pharmacol.* **2004**, *40*, 54–66.

(17) Nakatsuru, Y.; Wakabayashi, K.; Fujii-Kuriyama, Y.; Ishikawa, T.; Kusama, K.; Ide, F. Dibenzo[a,l]pyrene-induced genotoxic and carcinogenic responses are dramatically suppressed in aryl hydrocarbon receptor-deficient mice. *Int. J. Cancer* **2004**, *112*, 179–183.

(18) Maron, D. M.; Ames, B. N. Revised methods for the *Salmonella* mutagenicity test. *Mutat. Res.* **1983**, *113*, 173–215.

(19) Tsutsumi, T.; Amakura, Y.; Nakamura, M.; Brown, D. J.; Clark, G. C.; Sasaki, K.; Toyoda, M.; Maitani, T. Validation of the CALUX bioassay for the screening of PCDD/Fs and dioxine-like PCBs in retail fish. *Analyst* **2003**, *128*, 486–492.
(20) Mimura, J.; Yamashita, K.; Nakamura, K.; Morita, M.; Takagi, T. N.; Nakao, K.; Ema, M.; Sogawa, K.; Yasuda, M.; Katsuki, M.; Fujii-Kurimura, T. Loss of teratogenic response to 2,3,7,8-tetrachlorodibenzo-*p*-dioxin (TCDD) in mice lacking the Ah (dioxin) receptor. *Genes Cells* **1997**, *2*, 645–654.
(21) Marino, F.; Cecinato, A.; Siskos, P. A. Nitro-PAH in ambient particulate matter in the atmosphere of Athens. *Chemosphere* **2000**, *40*, 533–537.
(22) Nisbet, C.; LaGoy, P. Toxic Equivalency Factors (TEFs) for polycyclic aromatic hydrocarbons (PAHs). *Reg. Toxicol. Pharmacol.* **1992**, *16*, 290–300.
(23) Papageorgopoulou, A.; Manoli, E.; Touloumi, E.; Samara, C. Polycyclic aromatic hydrocarbons in the ambient air of Greek towns in relation to other atmospheric pollutants. *Chemosphere* **1999**, *39*, 2183–2199.
(24) Lodovici, M.; Venturini, M.; Marini, E.; Grechi, D.; Dolara, P. Polycyclic aromatic hydrocarbons air levels in Florence, Italy, and their correlation with other air pollutants. *Chemophere* **2003**, *50*, 377–382.
(25) Fernandez-Salguero, P. M.; Hilbrt, D. M.; Rudikoff, S.; Ward, J. M.; Gonzalez, F. J. Aryl-hydrocarbon receptor deficient mice are resistant to 2,3,7,8-tetrachlorodibenzo-*p*-dioxin toxicity. *Toxicol. Appl. Pharmacol.* **1996**, *140*, 173–179.
(26) Kondraganti, S. R.; Fernandez-Salguero, P.; Gonzalez, F. J.; Ramos, K. S.; Jiang, W.; Moorthy, B. Polycyclic aromatic hydrocarbon-inducible DNA adducts: Evidence by ^{32}P-Post-labeling and use of knockout mice for Ah receptor-independent mechanisms of metabolic activation in vivo. *Int. J. Cancer* **2003**, *103*, 5–11.
(27) Galvan, N.; Jaskula-Sztul, R.; MacWilliams, P. S.; Czuprynski, C. J.; Jefcoate, C. R. Bone marrow cytotoxicity of benzo[a]pyrene is dependent on CYP1B1 but is diminished by Ah receptor-mediated induction of CYP1A1 in liver. *Toxicol. Appl. Pharmacol.* **2003**, *193*, 84–96.
(28) Uno, S.; Dalton, T. P.; Dragin, N.; Curran, C. P.; Derkenne, S.; Miller, M. L.; Shertzer, H. G.; Gozalez, F. J.; Nebert, D. W. Oral Benzo[a]pyrene in CYP1 Knockout Mouse Lines: CYP1A1 Important in Detoxication, CYP1B1 Metabolism Required for Immune Damage Independent of Total-Body Burden and Clearance Rate. *Mol. Pharmacol.* **2006**, *69*, 1103–1114.
(29) Nesnow, S.; Ross, J. A.; Mass, M. J.; Stoner, G. D. Mechanistic relationships between DNA adducts, oncogene mutations and lung tumourigenesis in strain A mice. *Exp. Lung Res.* **1998**, *24*, 395–405.
(30) Grimmer, G.; Brune, H.; Deutsch-Wenzel, R.; Naujack, K. W.; Misfeld, J.; Timm, J. On the contribution of polycyclic aromatic hydrocarbons to the carcinogenic impact of automobile exhaust condensate evaluated by local application onto mouse skin. *Cancer Lett.* **1983**, *21*, 105–113.
(31) Grimmer, G.; Brune, H.; Deutsch-Wenzel, R.; Dettbarn, G.; Misfeld, J. Contribution of Polycyclic Aromatic Hydrocarbons to the Carcinogenic Impact of Gasoline Engine Exhaust Condensate Evaluated by Implantation into the Lung of Rats. *J. Natl. Cancer Inst.* **1984**, *72*, 733–739.
(32) Grimmer, G.; Brune, H.; Deutsch-Wenzel, R.; Dettbarn, G.; Misfeld, J. Contribution of Polycyclic Aromatic Hydrocarbons and Polar Polycyclic Aromatic Compounds to the Carcinogenic Impact of Flue Gas Condensate from Coal-Fired Residential Furnaces Evaluated by Implantation into the Rat Lung. *J. Natl. Cancer Inst.* **1987**, *78*, 935–941.
(33) Grimmer, G.; Brune, H.; Deutsch-Wenzel, R.; Dettbarn, G.; Jacob, J.; Naujack, K.-W.; Mohr, U.; Ernst, H. Contribution of polycyclic aromatic hydrocarbons and nitro-derivatives to the carcinogenic impact of diesel engine exhaust condensate evaluated by implantation into the lungs of rats. *Cancer Lett.* **1987**, *37*, 173–180.
(34) Casellas, M.; Fernandez, P.; Bayona, J. M.; Solanas, A. M. Bioassay-directed chemical analysis of genotoxic components in urban airborne particulate matter from Barcelona (Spain). *Chemosphere* **1995**, *30*, 725–740.
(35) Grimmer, G.; Brune, H.; Deutsch-Wenzel, R.; Dettbarn, G.; Misfeld, J.; Abel, U.; Timm, J. The contribution of polycyclic aromatic hydrocarbons to the carcinogenic impact of emission condensate from coal-fired residential furnaces evaluated by topical application to the skin of mice. *Cancer Lett.* **1984**, *23*, 167–176.
(36) Arlt, V. M.; Hewer, A.; Sorg, B. L.; Schmeiser, H. H.; Phillips, D. H.; Stiborova, M. 3-Aminobenzanthrone, a human metabolite of the environmental pollutant 3-nitrobenzanthrone, forms DNA adducts after metabolic activation by human and rat liver microsomes: Evidence for activation by cytochrome P450 1A1 and P450 1A2. *Chem. Res. Toxicol.* **2004**, *17*, 1092–1101.
(37) Stiborova, M.; Dracinska, H.; Hajkova, J.; Kaderabkova, P.; Frei, E.; Schmeiser, H. H.; Soucek, P.; Phillips, D. H.; Arlt, V. M. The environmental pollutant and carcinogen 3-nitrobenzanthrone and its human metabolite 3-aminobenzanthrone are potent inducers of rat hepatic cytochromes P450 1A1 and -1A2 and NAD(P)H:quinone oxidoreductase. *Drug Metab. Dispos.* **2006**, *34*, 1398–1405.
(38) Revel, A.; Raanani, H.; Younglai, E.; Xu, J.; Rogers, I.; Han, R.; Savouret, J. F.; Casper, R. F. Resveratrol, a Natural Aryl Hydrocarbon Receptor Antagonist, Protects Lung from DNA Damage and Apoptosis Caused by Benzo[a]pyrene. *J. Appl. Toxicol.* **2003**, *23*, 255–261.

Received for review November 24, 2006. Revised manuscript received February 21, 2007. Accepted February 26, 2007.

ES062793G

BIOCHEMICAL PHARMACOLOGY 74 (2007) 256–264

available at www.sciencedirect.com

ScienceDirect

journal homepage: www.elsevier.com/locate/biochempharm

β-Cryptoxanthin, a novel natural RAR ligand, induces ATP-binding cassette transporters in macrophages

Akira Matsumoto[a,b], *Hajime Mizukami*[b], *Satoshi Mizuno*[c], *Keizo Umegaki*[d], *Jun-ichi Nishikawa*[e], *Koichi Shudo*[f], *Hiroyuki Kagechika*[g], *Makoto Inoue*[a,b,*]

[a] *Laboratory of Medicinal Resources, School of Pharmacy, Aichi Gakuin University, 1-100 Kusumoto-cho, Chikusa-ku, Nagoya 464-8650, Japan*
[b] *Laboratory of Pharmacognosy, Graduate School of Pharmaceutical Sciences, Nagoya City University, 3-1 Tanabe-dori, Mizuho-ku, Nagoya 467-8603, Japan*
[c] *Research and Development of Kemin Health Co. Ltd., 600 E. Court Ave., Suite A Des Moines, IA 50309, USA*
[d] *Information Center, National Institute of Health and Nutrition, 1-23-1 Toyama, Shinjuku-ku, Tokyo 162-8636, Japan*
[e] *Laboratory of Environmental Biochemistry, Graduate School of Pharmaceutical Sciences, Osaka University, 1-6 Yamada-oka, Suita, Osaka 565-0871, Japan*
[f] *Research Foundation Itsuu Laboratory, 2-28-10 Tamagawa, Setagaya-ku, Tokyo 158-0094, Japan*
[g] *School of Biomedical Science, Tokyo Medical and Dental University, 2-3-10 Kanda-Surugadai, Chiyoda-ku, Tokyo 101-0062, Japan*

ARTICLE INFO

Article history:
Received 18 January 2007
Accepted 16 April 2007

Keywords:
β-Cryptoxanthin
Lutein
Xanthopyll
Retinoic acid receptor
Retinoid X receptor
ATP-binding cassette transporter

ABSTRACT

Despite its serious adverse effects, recent accumulating evidence suggests that a physiological retinoic acid receptor (RAR) agonist, all-*trans* retinoic acid (atRA), exhibits preventive effects on atherogenesis. Therefore, the present study was designed to explore novel natural RAR ligands with anti-atherogenic effects in order to identify and develop a drug without severe side effects. Among xanthophylls and carotenoids studied, β-cryptoxanthin and lutein exhibited RAR ligand activity in yeast two-hybrid system that was found to be completely abolished by the RAR pan-antagonist LE540. Furthermore, these molecules can bind the RAR ligand-binding domain in the CoA-BAP system but not RXR ligand-binding domain. These results indicate that both β-cryptoxanthin and lutein serve as ligands for RAR, but not RXR, although their binding affinity was three orders of magnitude lower than that of atRA. Additionally, when applied to macrophages, β-cryptoxanthin indeed was found to induce the ATP-binding cassette transporter A1 (ABCA1) and ABCG1 mRNAs, which exert anti-atherosclerotic effects by preventing cholesteryl ester accumulation in macrophages. The induction of ABCA1 proteins by β-cryptoxanthin as well as atRA was abrogated by LE540. In summary, β-cryptoxanthin appears to be more an efficient provitamin A source than other carotenoids and xanthophylls including β-carotene, since β-cryptoxanthin can act not only as a RAR agonist but also a source of vitamin A. Taking into account that the pharmacodynamics difference between β-cryptoxanthin and atRA, β-cryptoxanthin appears to exert beneficial effects on atherogenesis through RAR activation in the manner different from atRA.

© 2007 Elsevier Inc. All rights reserved.

* *Corresponding author at:* Laboratory of Medicinal Resources, School of Pharmacy, Aichi Gakuin University, 1-100 Kusumoto-cho, Chikusa-ku, Nagoya 464-8650, Japan. Tel.: +81 52 757 6792; fax: +81 52 757 6793.
E-mail address: minoue@dpc.aichi-gakuin.ac.jp (M. Inoue).
0006-2952/$ – see front matter © 2007 Elsevier Inc. All rights reserved.
doi:10.1016/j.bcp.2007.04.014

1. Introduction

Prospective cohort studies show a direct inverse association between a higher intake of fruits and vegetables and the development of cardiovascular diseases, such as coronary heart disease and stroke [1–4]. Among major carotenoids and xanthophylls, such as β-carotene, lycopene, α-carotene, lutein, and β-cryptoxanthin, β-carotene has been studied most extensively, but no benefits have been found for it in randomized trials [5,6]. These studies indicate that the apparent benefits from fruit and vegetable intake are not due to β-carotene itself and may be more properly ascribed to other nutrients or other factors present in these foods.

Atherosclerosis is a complex disease characterized by chronic inflammation [7] and by abnormal and excessive proliferation of vascular smooth muscle cells (VSMCs) [8]. In addition, the presence of activated macrophages and T cells in lesions caused by the disease suggest that cell-mediated immune reactions also occur during the development of atherosclerosis [9]. All-*trans* retinoic acid (atRA), a bioactive retinoic acid produced from vitamin A (retinol), is known to inhibit neointimal formation following balloon withdrawal injury of rat [10–12] or rabbit carotid artery [13]. atRA is also capable of inhibiting VSMC proliferation and promoting VSMC differentiation [14–16]. In regards to macrophages that are intimately involved in atherosclerosis development, atRA has been shown to induce ATP-binding cassette transporter A1 (ABCA1) [17] and a synthetic retinoid (AM80) reduced scavenger receptor expression [18], suggesting that atRA or its derivatives prevent foam cell formation by decreasing intracellular cholesteryl ester accumulation [19]. In addition, it was recently been reported that atRA exerts direct effects on T cells by suppressing T helper (T_h)1 development and enhancing T_h2 development that is essential for antibody responses [20,21]. Since the T_h1-driven immune response has been consistently shown to promote atherosclerosis, immunomodulation through T_h2 should be suitable to help reduce the progression of atherosclerosis. In total, these findings imply that atRA may be capable of attenuating the development of atherosclerosis by suppressing cellular immunity and stimulating humoral immunity.

To date, no clinically proven therapy exists for the successful management of neointimal formation in atherosclerosis or restenosis following angioplasty. However, atRA therapy appears to be a promising attractive approach for the treatment of neointimal formation especially given the clinical applications of atRA have been shown to have some success in the treatment of human diseases such as cancer, psoriasis, and leukemia. However, the therapeutic use of atRA has been excluded from consideration because of serious adverse effects such as skin or liver toxicity, teratogenesis, hypertriglyceridemia and development of resistance to atRA in addition to atRA syndrome characterized by fever, respiratory distress, interstitial pulmonary infiltrates, pleural and pericardial effusion, episodic hypotension, and acute renal failure [22,23].

Retinoid signaling is transduced by two families of nuclear receptors, the retinoic acid receptor (RAR), and the retinoid X receptor (RXR) [24,25]. These receptors belong to the superfamily of nuclear hormone receptors that act as ligand-activated transcription factors. RAR forms a heterodimer with RXR and the ligand–receptor complexes act as inducible transcription regulators of several genes by binding to specific retinoic acid response element. The pleiotropic effects of retinoids are primarily brought about by the existence of two families receptors (RAR and RXR), the RAR isotypes (α, β, and γ), and the RXR isotypes (α, β, and γ) in addition to the cross-talk of these receptors with other signaling pathways and the existence of multiple putative coactivators and corepressors [26]. In addition, since the RAR ligand-binding domain is capable of adopting a conformation exhibiting a large hydrophobic cavity similar to that observed in PPARγ-ligand-binding domain [27], various RAR ligands can induce various conformational changes in RAR, resulting in versatile gene expression and repression via the recruitment of different coactivators or corepressors as PPARγ ligands [28,29]. Furthermore, metabolic enzymes and retinoid binding proteins involved in storage, transport, uptake and sequestration of retinoids play critical roles in determining the availability of bioactive retinoids in cells [30]. This notion may indicate that RAR ligands that are metabolically different from the natural ligands for the RAR, such as atRA, 9-*cis*-RA, and 13-*cis*-RA [31], appear to be useful in treating various diseases.

Consequently, it seems to be very important to explore various RAR ligands that can create beneficial responses in a living body in order to develop therapeutic agents for cancer, atherosclerosis, and rheumatoid arthritis while simultaneously clarifying the signaling pathways associated with RAR. The present study was designed to search for natural RAR ligands among carotenoids and xanthophylls in order to develop potential therapeutic agents for cardiovascular diseases and to clarify the benefits of fruit and vegetable intake to prevent such diseases. That research had culminated in the identification of β-cryptoxanthin as a novel natural RAR agonist and a better provitamin A to activate RAR/RXR heterodimer than β-carotene.

2. Materials and methods

2.1. Chemicals and reagents

β-Cryptoxanthin, zeaxanthin, β-carotene, lycopene, all-*trans* retinoic acid, and 9-*cis* retinoic acid were obtained from Yashima Pure Chemical Co. Ltd. (Tokushima, Japan), Extrasyntheses (Genay, France), Nacalai Tesque Co. (Kyoto, Japan), Wako Pure Chemical Industries (Osaka, Japan), Sigma Chemical Co. (St. Louis, USA), and Sigma Chemical Co. (St. Louis, USA), respectively. Lutein was kindly provided from Koyo Mercantile Co. Ltd. (Tokyo, Japan). RAR antagonist, LE540, was kindly provided from Dr. Kagechika of Tokyo Medical and Dental University. All test chemicals were dissolved in dimethylsulfoxide (DMSO) (Nacalai Tesque, Kyoto, Japan) and stored at −80 °C until use. Antibody against ABCA1 was kindly provided from Dr. Yokoyama of Medical School of Nagoya City University.

2.2. Animals

Male C57BL/6J mice (6–8 weeks of age) were purchased from Nippon Charles River (Kanagawa, Japan). All animals were

kept in a temperature-controlled room (23 ± 1 °C) with a 12 h light/dark cycle, under specific-pathogen-free conditions and given a sterilized commercial diet (CE-2; Nippon Crea Co., Ltd., Shizuoka, Japan) and water *ad libitum* at the Laboratory Animal Center of Nagoya City University. All animal procedures were approved by the institutional animal care and use committee of Nagoya City University.

2.3. Yeast two-hybrid assay

Yeast expressing GAL4DBD-RARα or γ, GAL4DBD-RXRγ, GAL4AD-TIF2, and *lacZ* reporter plasmids were kindly provided by Dr. Nishikawa of Osaka University [32]. Yeast transformants were grown overnight at 30 °C with vigorous shaking in 5 ml of selective medium without leucine and tryptophan. The yeast was harvested by a centrifugation at 3000 × *g* for 15 min and suspended in fresh medium. The absorbance at 630 nm of the cell suspension was measured with U-2001 spectrophotometer (Hitachi High-Technologies Co., Tokyo, Japan). All assays were performed by using the yeast suspension with the absorbance at 630 nm of 0.6. Four hundred and fifty microliters aliquots of the yeast suspension were cultured in the presence of 5 μl of test compounds for 4 h at 30 °C with vigorous shaking. The 100 μl of chemically treated yeasts were incubated with 30 μl of Z buffer (0.1 M sodium phosphate (pH 7.9), 10 mM KCl, 1 mM $MgSO_4$) containing 4 mg/ml ZYMOLYASE®-20T (Seikagaku Co., Tokyo, Japan) for 30 min at 30 °C. The enzymatic reaction of β-galactosidase was initiated by the addition of 25 μl of 0.5 mg/ml chlorophenol Red β-D-galactopyranoside dissolved in 0.1 M sodium phosphate buffer (pH 7.9). When the red color developed, 50 μl of 2 M Na_2CO_3 were added to stop the reaction. The absorbances at 540 and 630 nm were measured and the activity was calculated according to the following equation: U = [(absorbance at 540 nm) − (absorbance at 630 nm)]/(absorbance at 630 nm at the start of the assay). β-Galactosidase activity is presented as the means ± S.D. of three determinations.

2.4. Binding assay using CoA-BAP system [33]

Binding assay was performed using Nu ligand kit (Microsystems, Kyoto, Japan) according to the manufacturer's instructions. Briefly, 100 μl of GST-fused nuclear receptor protein dissolved in 0.1 M sodium carbonate buffer (pH 6.8) was added to 96-well plate and incubated overnight at 4 °C. After washing the plate with 120 μl of wash buffer A, alkaline phosphatase-fused TIF2 protein dissolved in wash buffer A and test compounds dissolved in DMSO were added and incubated for 1 h at 4 °C. The plate was then washed with 120 μl of wash buffer B. The enzyme reaction was started at 30 °C by the addition of 100 μl of NPP solution. When the yellow color developed, the reaction was stopped by the addition of 25 μl of 0.5 M NaOH. The absorbance at 405 nm was measured with ARVO™ Wallac 1420 Multilabel Counter (Wallac, Finland).

2.5. Cell culture

Thioglycolate-elicited macrophages were prepared as previously described [34]. Briefly, C57BL/6J mice were intraperitoneally injected with 2 ml of 3% thioglycolate medium (Difco Laboratories, Detroit, MI, USA). Six days later, peritoneal macrophages were harvested from the abdominal cavity, seeded at a concentration of 2 × 10^6 cells/ml and maintained in RPMI1640 medium (Invitrogen, CA, USA) supplemented with 10% fetal bovine serum (FBS), 100 U/ml of penicillin (Invitrogen), and 100 μg/ml of streptomycin (Invitrogen) for 2 h. After non-adherent cells were removed, the resulting macrophages were incubated with various concentrations of the test compounds in RPMI1640 medium supplemented with 0.1% bovine serum albumin for 8 and 20 h in order to prepare mRNA and protein fraction, respectively.

2.6. Western blot analysis

After 20 h incubation, macrophages were harvested and lysed by homogenization in 80 μl of lysis buffer containing 10 mM Tris-base, pH 8.0, 0.1% Triton X-100, 0.15 mM KCl, 5 mM mercaptoethanol, 1.3 mM EDTA, and protease inhibitor cocktail tablets (Roche Diagnostics) on ice. The lysates were palletized by centrifugation (12,000 × *g*, 15 min) at 4 °C, and the supernatant was assayed for protein concentration (Bradford method, Bio-Rad Laboratories). The lysates (protein 30 μg) were suspended in 0.9 M urea, 0.2% (v/v) Triton X-100, and 0.1% (w/v) dithiotheitol and supplied with 10% (w/v) lithium dodecylsulfate and then separated by 8% LDS-PAGE followed by transferring onto a polyvinylidene fluoride membrane (Millipore) in a transfer buffer (25 mM Tris, 192 mM glycine, 0.02% SDS, 20% methanol). The membrane was blocked for 3 h in a solution of 5% powdered skim milk in Tris-buffered saline (TBS) and then incubated with anti-ABCA1 antibody diluted 1:1000 in TBS containing 1% of skim milk and 0.05% Tween-20 overnight at 4 °C. The blot was washed in three changes of wash buffer (0.05% Tween-20 in TBS) and then incubated with alkaline phosphatase-conjugated anti-rabbit IgG antibody (Cell Signaling Technology, MA, USA) in 1% powdered skim milk and 0.05% Tween-20 in TBS for 1 h at room temperature. The blot was thoroughly washed in three changes of wash buffer, and ABCA1 was detected using CDP-Star (PE Biosystems, Bedford, MS, USA) as a substrate of alkaline phosphatase. Protein concentration was determined using LAS-3000mini (FUJIFILM, Tokyo, Japan).

2.7. Reverse transcription

After 8 h incubation, macrophages were harvested and total RNA from macrophages was extracted using a RNeasy™ mini kit (Qiagen K.K., Tokyo, Japan) according to the manufacturer's instruction. The resulted RNA was treated with DNase I (Invitrogen) to degrade contaminating DNA. The RNA was dissolved in diethyl pyrocarbonate-treated water and quantified by GeneQuant II (GE Healthcare Bio-Science Corp., NJ, USA). To prepare first strand cDNA, 500 ng of total RNA was reverse-transcribed using Revertra Ace (Toyobo Biochemicals, Tokyo, Japan) according to the manufacturer's instructions.

2.8. Quantitative RT-PCR

Reactions were prepared in 96-well optical grade PCR plate in a total of 50 μl containing the following components; 33 μg of cDNA dissolved in 25 μl of water, 25 μl of 2× TaqMan™ Universal Master Mix, 2.5 μl of TaqMan™ gene expression assays containing fluorogenic probes predesigned at Applied

Biosystems. Thermal cycling conditions consisted of an initial step of 2 min at 50 °C and then 10 min at 95 °C, followed by 40 cycles of 15 S at 95 °C and 1 min at 60 °C for ABCA1, ABCG1, and β-actin. Adjustments for baseline and threshold were performed according to the manufacturer's instructions. Levels of ABCA1 and ABCG1 mRNA expression were subsequently normalized relative to β-actin mRNA levels and calculated with delta–delta Ct method.

2.9. Statistical analysis

Data was represented as the mean ± S.D. or S.E. as described in the legends. Statistical significance was determined by Dunnett's test using Stat Light software. P-values less than 0.05 were considered significant.

3. Results

3.1. RAR ligand activity using yeast two-hybrid assay

The results of the binding activity against RARα and γ for the carotenoids and xanthopylls evaluated are shown in Fig. 1 for the yeast two-hybrid assay described in Section 2. atRA showed dose-dependent increase in β-galactosidase activity at the concentration of 10^{-10} to 10^{-8} M (Fig. 2A). Among carotenoids and xanthophylls tested, β-cryptoxanthin exhibited a dose-dependent increase in β-galactosidase activity in the concentration of 10^{-7} to 10^{-5} M. Lutein also showed increased β-galactosidase activity but at higher concentrations than β-cryptoxanthin. In contrast, β-carotene, zeaxanthin, astaxanthin, and lycopene did not exhibit significant activity. The transcription activation by β-cryptoxanthin and lutein was observed in both RARα and RARγ assays. When the agonist activity against RXRγ, which forms the heterodimer with RAR and transduces the signal, was determined, no activity was detected among any of the carotenoids and xanthophylls tested (Fig. 2B).

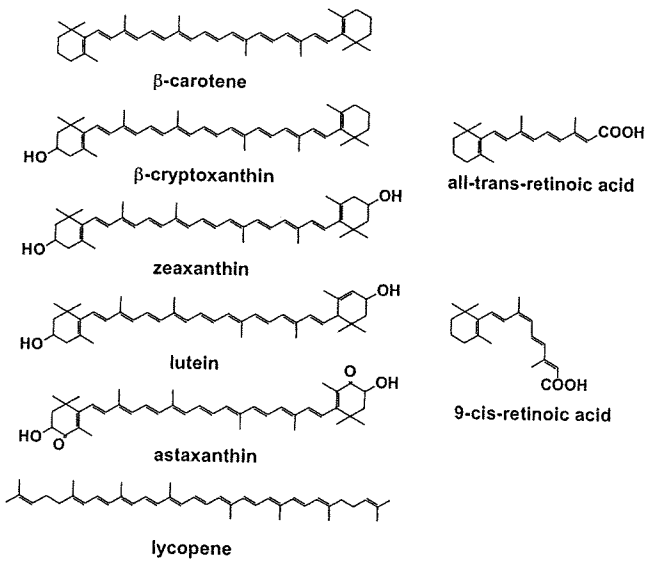

Fig. 1 – Structures of xanthophylls, carotenoids, and retinoic acid used in the present study.

3.2. Effect of RAR pan-antagonist LE540 on RAR binding activity of β-cryptoxanthin and lutein

To confirm whether β-galactosidase was induced by β-cryptoxanthin and lutein via RARα or RARγ, the effect of LE540, which is a pan-antagonist for RARs [35], was investigated. As shown in Fig. 3, β-cryptoxanthin induced β-galactosidase activity at the concentrations of 0.1 and 1 μM. This induction was completely inhibited by 10 μM LE540. Lutein induced β-galactosidase activity at 1 μM concentration and 10 μM LE540 abolished that induction. These results indicate that both β-cryptoxanthin and lutein induce β-galactosidase via RARα or γ in this yeast two-hybrid assay.

3.3. Binding assay for RAR using CoA-BAP system

To assess the agonist activity of β-cryptoxanthin and lutein and to preclude the possibility that β-cryptoxanthin metabolites or degradation products by yeast bind RARs, the binding activity to RAR was evaluated using the cell-free CoA-BAP system [33]. β-Cryptoxanthin and lutein were found to bind RARα in agreement with the result obtained in yeast two-hybrid assay. Conversely, zeaxanthin did not exhibit comparable binding activity in the CoA-BAP systems (Fig. 4) as was found in yeast two-hybrid assay. The β-cryptoxanthin dose where the binding activity was detected was three orders of magnitude higher than that of atRA. Additionally, when the binding activity to RXR was measured, no activity was found in β-cryptoxanthin and lutein. This corresponds to the results obtained from the yeast two-hybrid assay.

3.4. Effect of β-cryptoxanthin on ATP-binding cassette transporters in macrophages

Recently, ATP-binding cassette transporters A1 (ABCA1) and ABCG1 were reportedly induced in macrophages following the activation of RAR/RXR by retinoic acid [17]. To verify that β-cryptoxanthin acts as an RAR agonist in cells, the capacity of β-cryptoxanthin to induce ABCA1 and ABCG1 mRNAs in macrophages was evaluated. As shown in Fig. 5, β-cryptoxanthin increased mRNA levels of ABCA1 and ABCG1 dose-dependently, although the levels were less than those induced by atRA. Furthermore, the concentrations needed to induce both mRNAs were very similar to those found to induce effects in the yeast two-hybrid assay as well as in the CoA-BAP system. When ABCA1 protein levels were assessed by Western blot analysis, β-cryptoxanthin increased protein levels compared with vehicle-treated group, but less than atRA (Fig. 6A). In addition, the induction of ABCA1 protein by β-cryptoxanthin (5 μM) as well as atRA (5 μM) was completely abrogated by LE540 treatment (Fig. 6B). However, β-cryptoxanthin was not capable of increasing ABCG1 protein, although it increased ABCG1 mRNA levels (data not shown).

4. Discussion

In the present study, it has clearly demonstrated that β-cryptoxanthin and lutein, which are major nutrients in fruits and vegetables, are novel natural ligands for RARs and that β-